Response to review

The reviewer's comments are given below in black font and our responses are in green font. A full tracked changes version of the manuscript is at the end of this document. Note also in responding to the reviewers comments (details below) we have also added 7 references.

Reviewer #1:

Review of "Onshore and Offshore Wind Resources and Operating Conditions in the Eastern U.S." by Rebecca Foody, Jacob Coburn, Jeanie A. Aird, Rebecca J. Barthelmie and Sara C. Pryor

This study describes the statistical analysis of a comprehensive lidar data set with focus on onshore and offshore wind speeds and power production in the U.S.

The data set described in this manuscript is interesting and of high relevance for wind energy research. The thematic itself is within the scope of the journal. However, a clear structure is missing, I could not identify clear objectives and/or hypotheses to be addressed and there is a lack of clear interpretations, discussions, and conclusions. The reader often needs either to accept statements without a clear proof or need to interpret the results by its own. Therefore, I recommend a major revision of the manuscript.

Response: We regret that the reviewer did not find our structure clear. We felt that by writing in the paragraph starting on line 51 'We evaluate four aspects of the wind power generation potential on- and offshore:' and then listing them that we were setting out the objectives clearly. But in light of your concerns, we have completely restructured the introduction.

We have also changed the title to help the reader immediately know the purpose of the manuscript the new title is **Quantitative Comparison of Power Production and Power Quality Onshore and Offshore: A Case Study from the Eastern U.S.**

Specific comments

Introduction:

Entire Introduction: To my opinion, the big picture is missing here. What do you expect to find from the analyses. What do you want to explain or proof, what is your scientific question, the overall goal of your study?

We have re-written the introduction to read (quoting from the revised manuscript):

'Here we focus on the first of these reasons, and specifically seek to quantify the potential benefit of offshore wind turbine deployments using analyses of uniquely detailed wind profiles from an onshore LiDAR (Light Detection And Ranging) network and an offshore LiDAR network. We use these data sets to quantify and compare three aspects of the wind power generation potential on- and offshore:

1 Wind resource and power production. We present Weibull probability distribution parameters and derive energy density from the wind speed time series and compare and contrast the inferred wind resource at the onshore and offshore sites. We further compute and compare the Annual Energy Production (AEP) from the time series of wind speeds at each LiDAR site using a common wind turbine power curve.
2 Power quality. Intermittency is frequently cited as a barrier to increased wind power integration into the electrical grid (Bistline and Blanford, 2021). We quantify and compare the frequency of zero power production and intensity and probability of so-called ramp events (i.e., rapid changes in wind speed and power production) (DeMarco and Basu, 2018;Pichault et al., 2021) from each onshore and offshore site where LiDARs have been deployed.
3 Predictability and persistence of wind speeds and power production (Haghi et al., 2013;Haslett and Raftery, 1989). Within liberalized electricity markets, wind farm owner/operators bid in advance (e.g. 24 hours in advance) and are charged penalties for any imbalance between the bid

and actual production (Pinson et al., 2007). Hence, accurate forecasts of wind generation are important to reduce penalties and maximize revenue (Barthelmie et al., 2008). Persistence models where the power production at some future time is modeled as a function of power production in the recent past is often used as a benchmark forecast against which more sophisticated short-term power production models are compared (Kariniotakis et al., 2004). Also many statistical short-term forecast models are predicated in part on persistence (Zeng and Qiao, 2011) and thus are most skillful when the power production time series exhibits high temporal autocorrelation. We quantify the temporal autocorrelation of power production from each onshore and offshore site and compare the degree to which electrical power production from the onshore and offshore locations differ with respect to persistence and short-term predictability.

We further use these LiDAR measurements to quantify and compare a key driver of wind turbine loading at the on- and off-shore locations:

4 Extreme or anonymous wind shear across the rotor plane. Low-Level Jets (LLJ) are confined wind speed maxima within the lower atmospheric boundary layer (Stensrud, 1996) and are associated with enhanced vertical wind speed (and sometimes directional) shear relative to typical near-logarithmic profiles. LLJ within the wind turbine rotor plane are associated with higher aerodynamic and structural loading (Gutierrez et al., 2019;Gadde et al., 2021). Analyses of simulations with the Weather Research and Forecasting (WRF) model suggest that offshore coastal regions of the U.S. mid-Atlantic (including the locations of the buoys from which data are presented) generally exhibit a weakly sheared profile across the rotor plane and a relatively low frequency of LLJ (Aird et al., 2022). That analysis found LLJ in the lowest 500 m of the atmosphere are most frequent south of Massachusetts and during the summer (8% of all hours). They frequently occur at heights that intersect the wind turbine rotor plane, and at wind speeds within typical wind turbine operating ranges. Further, LLJ diagnosed from the WRF output were most intense and have lowest elevation under strong horizontal temperature gradients and lower planetary boundary layer heights. For comparative purposes, data from the NYSM LiDARs are used here to evaluate wind shear across the rotor plane and the occurrence, intensity, and height of LLJ at the onshore locations.

We also analyze the LiDAR data to quantify two other properties of relevance to wind energy integration into the electricity generation supply:

5 Co-variation of wind speeds and power production with varying distance separation (Pryor et al., 2014;Solbrekke et al., 2020). The electric power transmission network in the contiguous U.S. comprises three main interconnections (eastern, western, and Electric Reliability Council of Texas (ERCOT)) and 66 'balancing authorities' that oversee regional operation of the electric grid and are referred to as Regional Transmission Operators (RTOs) or Independent System Operators (ISOs). New York (NY) state currently operates as a single state ISO. NY is both a net importer of electricity and the third most efficient state in terms of energy use per U.S. dollar of economic activity (https://www.eia.gov/state/analysis.php?sid=NY). Careful planning of wind farm locations on and offshore could ensure stable supply of wind-generated electricity into the grid and thus aid the transition from electricity imports and a current dependence on nuclear and natural gas (Eryilmaz et al., 2020). Here we quantify the spatial autocorrelation of power production from each onshore and offshore site where the LiDARs have been deployed to evaluate the decorrelation distance and hence provide guidance regarding optimal spatial scale of wind farm separation (on- and off-shore) for stability of wind power supply.

6 Seasonality and diurnal variability of wind power production (WPP) on- and off-shore for demand matching. Electricity demand varies with the level of economic activity and seasonal heating/cooling requirements which are a function of the regional climate (Castillo et al., 2022;Staffell and Pfenninger, 2018). Generally, electricity demand in the U.S. is minimized

between approximately 0400 and 0600 local time (LT), is high between 0800 and 1600 LT, and peaks between 1800 and 2100 LT (Burleyson et al., 2021). Diurnal variability of wind power generation is a function of location and land use but, for example, in ERCOT is highest at night (Kiviluoma et al., 2016), consistent with the expectation based on day-time variations in atmospheric stability caused by changes in net radiation and the surface energy balance. Because the oceans have higher specific heat capacity than land, this scale of variability is typically not present in the far offshore (> 20 km from the coast) (Barthelmie et al., 1996). At the seasonal scale, wind resources and power production in the midlatitudes and specifically the contiguous U.S. tend to peak in between October and April and are lowest in July or August due to pronounced shifts in the storm track and the frequency and intensity of mid-latitude cyclones (Pryor et al., 2020b). Recent research suggests WPP is highest in southeastern Canada and the northeastern U.S. during January and February (Coburn and Pryor, 2023). Thus, finally, we quantify whether electrical power from wind turbines deployed offshore exhibit higher or lower temporal matching with electricity demand in New York state at both the diurnal and seasonal scales.'

We feel this is a very clear statement of objectives, justification of the objectives and hope the reviewer concurs.

Page 2, line 51: The authors mention that there are few previous studies without giving any references. I would also recommend to shortly summarize what has been done and found in those few studies.

We actually couldn't find any comparable studies but did not want to preclude the possibility that such studies exist, but since we could not find a comparable studies we have dropped this statement.

Page 2, Point 1: I would expect a discussion/statement/explanation in the results part about the differences in the regions and what we can learn from it (e.g., an evaluation as to whether a region is more suitable as the others, beyond onshore-offshore differences)

We think the reviewer is referring to 'First, wind speeds tend to be higher and more consistent offshore due to both the lower surface roughness and lack of obstacles and topographic features that extract momentum and reduce both the wind speed and wind resource (Pryor and Barthelmie, 2002). Accordingly, Capacity Factors (CF), which are the ratio of actual power generation divided by the theoretical maximum power generation, are typically higher offshore. Data from operating wind farms in Denmark indicate CF from four offshore wind farms with installed capacity (IC) of 160 to 400 MW of 41-53% while CF from smaller onshore wind farms (IC: 16-70 MW) have CF of 28-41% (Enevoldsen and Jacobson, 2021). Within the U.S., the mean CF for onshore wind farms built between 2014 and 2019 is approximately 41% (Wiser et al., 2021). Simulations using numerical models for offshore wind energy lease areas along the U.S. east coast indicate CF above 46% largely as a result of the higher wind speeds offshore (Pryor et al., 2021;Barthelmie et al., 2023). '

It certainly is true that some regions of the world exhibit higher wind resources but our focus here is listing the factors that are responsible for 'Enhanced deployment of wind turbines offshore offers great promise in terms of enhanced renewable energy penetration into the electricity generation portfolio for three primary reasons'… So, respectfully, we are unconvinced that adding a discussion of the relative wind resource in different regions of the world would be useful here.

Page 2, line 79: I could not find a guidance regarding optimal special scale. I don't feel guided with only a short statement that correlation is lower than 0.4 for distances >350 km. I recommend using either another formulation or provide a more detailed and profound discussion in the results part.

Our apologies – the concept of the spatial decay of correlation and the e-folding distance may, indeed, not be widely understood. We have elaborated on this matter a little in the Methods. We have modified this sentence to read; 'Temporal autocorrelation coefficients of the power production time series are used to derive e-folding time scales (i.e. the time delay at which the correlation coefficient drops to e^{-1},

i.e. to 0.37) which is used to represent the time scale at which the system 'loses' the memory of the initial state (Wilks, 2011).'
(i.e. to add 0.37)
And then have added this sentence:
'The e-folding concept can also be applied in this context, to quantify the distance at the power production from two sites is no longer significantly correlated.'
So the bottom line is the separation distance at which the correlation coefficient for the power production time series from two sites two drops below about 0.37 (rounding to 0.4) is the distance at which the sites are no longer significantly correlated – or if you prefer if I wish to achieve a more stable electricity production through time I should place wind farms at sufficient separation that their individual generation is not significantly correlated. For this wind climate that distance is about 350 km.
We hope our changes to the text help to clarify that point.
Page 3, paragraph 1: There is quite a harsh transition from the previous paragraph and topics to this one. The topic is completely new, and I miss a kind of introduction to why this is important in your study and what you want to show/discuss with results to this. What is your goal, what do you want to compare and what are possible consequences for your major hypothesis? In this paragraph, you mention something from structural loading and wakes but what does it mean for whatever you want to show and where is the discussion about it in the results/conclusion part?
We regret you found this to be a harsh transition. Hopefully with the re-structure introduction you find the flow is smoother.
Page 3, paragraph 2: Wouldn't it be better to paste a goal at the beginning of a paragraph? Otherwise, there is again a harsh transition from one topic to another from which the reader initially has no idea what the reason is, where to focus on.
Again, we regret you found this to be a harsh transition. Hopefully with the re-structure introduction the flow is smoother. We do have an objective at the start of each bullet point.
Data Sources:
Page 4: The best year has a specific time frame for all positions, how about the analyses which are not based on the best years? Is the time span for all positions from January 2019 to December 2022 or are there some variabilities? If yes, how large are these and how would you expect them to influence your results?
There is always a compromise to be made – use all the data that you have in order to increase the sample size for statistical testing versus use the data period that best represents the seasonal cycle. This is indeed a challenge. So, for statistical testing where sample size aids confidence we use all records (e.g. spatial autocorrelation) but we also present to the reader information regarding how estimated AEP varies as a function of the data sample.
Methods:
Page 7, chapter 3.3: Which question shall be answered by an analysis of the wind profile and why are you using shear and LLJ? In what sense are LLJ of relevance to wind energy applications?
As we wrote:
'The International Electrotechnical Commission (IEC) 61400-1 standard states the expected value of α over land is 0.2 and is typically in the range of 0.05 to 0.25 and uses a value of 0.2 in the normal wind profile model (IEC, 2019). The occurrence of α beyond this range implies shear across the rotor plane differs from this design expectation and hence may indicate higher mechanical loading.
Thus on the most fundamental level we are seeking to report how frequently the shear is outside this expectation. The LLJ analysis is really to examine if one source of anomalous wind shear profiles (i.e. the frequency of LLJ) is higher/lower on and offshore.' We hope the modified introduction and the addition of an additional reference.

We have also added some text to the results section.: 'The implication is that large wind turbines deployed in these locations may experience a relatively high frequency of large unbalanced rotor loads and reduced component lifetimes unless such loads can be appropriately compensated (Hur et al., 2017).'

Page 7, lines 223-225: Is this a commonly used method? Do you have references for this method which show that this can be done for wind energy or similar purposes? I wonder how suitable this method is considering the lower spatial and temporal resolution of ERA-5 compared to measurements, the difference in time spans (comparing results from 44 years (ERA-5) to max 4 years (data) and the fact that ERA-5 has uncertainties on its own and additional uncertainties by the conversion from 10&100 m to 150 m. I would also suggest providing a kind of uncertainty or at least a discussion about this issue.

We believe the reviewer is referring to; 'Hourly values from the 40-year $U150_{ERA5}$ and $P150_{ERA5}$ record are randomly resampled 1000 times with replacement using the number of hours from each month that the LiDAR data are available (Figure 3). For each of these 1000 bootstrapped samples the annual mean wind speed and AEP is calculated to provide an estimate of uncertainty due to the short time series from the LiDARs.' Yes, bootstrap resampling is very frequently used to quantify confidence intervals around a metric (see for example the textbook by Dan Wilks or this text by Mudelsee; Climate Time Series Analysis: Classical Statistical and Bootstrap Methods (Atmospheric and Oceanographic Sciences Library, 51)). We have added a citation of the Wilks reference to the methods.

Perhaps the reviewer is speaking to our specific application. The mean power law coefficient 0.21 which for a height interval of 100 to 150 is equal to a correction of 0.06 (or if you prefer a multiplier of 1.09 on the 100-m wind speed) so it's a small correction. We have now clarified this in the text. In terms of bootstrap resampling to derive uncertainties on wind speeds per se, it is a generalizable statistical method that can be applied to any geophysical property (see the book by Mudelsee)

We have clarified what the purpose of this analysis is by adding this statement; 'This analysis explicitly acknowledges the presence of low-frequency variability (seasonal to multi-decadal) in mid-latitude wind speeds and wind resources (Pryor et al., 2020a) and is designed to quantify the uncertainty on mean wind speeds and power production computed from the relatively short LiDAR data time series. '

Results:

Page 8, lines 258-259: What does this mean? Why are low summer values a hint for a negative bias? Summer values are often lower, winter values often higher, so there are seasonal deviations from annual (and also long-term) mean values.

We regret this statement wasn't clearer. We have rewritten it to read:

'Bootstrapping of ERA5 data indicates the mean annual wind speed computed from the LiDAR time series at the NYSM sites is likely underestimated by ~ 1.5-4.5% while AEP is underestimated by ~3-10% due to the high data availability in summer.'

We hope this clarifies.

Page 8, lines 258-259: Definitely missing here is a detailed description and justification (preferably with reference) of how a long-term time series with relatively coarse resolution can lead to a meaningful error estimate of a point measurement, even more so when different time periods are used for this purpose. Why isn't it more likely here, that differences come from the interannual variability? What makes you believe that the data availability is responsible for these differences, in particular when you consider annual averages, and if so, wouldn't another way of calculating annual averages be the solution to avoid or at least minimize the influence? How do you calculate them that they have such a strong influence?

We regret any confusion – precisely we are examining inter-annual variability!. We hope we have removed any confusion by adding this statement in methods: 'Although the LiDAR data sets that we analyze here are – to our knowledge – unique in terms of the duration and number of sites considered, we also contextualize the results and inferences drawn from these multi-year, but relatively short duration, observations using the > 40 year duration ERA5 reanalysis product (Hersbach et al., 2020). This analysis explicitly acknowledges the presence of low-frequency variability (seasonal to multi-decadal) in mid-latitude wind speeds and wind resources (Pryor et al., 2020a) and is designed to quantify the uncertainty on mean wind speeds and power production computed from the relatively short LiDAR data time series. '

A minor note: If the cause is inter-annual variability due to differences in cyclone frequency/intensity that will be manifest in approximately equal magnitude in 'point' and spatially averaged values (unless the site is in complex terrain where directional channeling may be a factor).

Page 11: Concerning the differences in Weibull scale parameters and AEP between best year and all data: What is the conclusion of this finding? Interannual variability? Data under-/overrepresentation? Any proofs for the one or the other?

We did this analysis because it is important to acknowledge sources of uncertainty including incomplete time series. We note that in doing these analyses we also demonstrate that the on-shore off-shore differences are robust to data sampling issues. Accordingly, to avoid any confusion we have added the statement; 'It is important to note that the differences in energy density computed from the on-shore and off-shore LiDAR data sets are robust to these sampling issues.'

Page 12, lines 290-293: A description/interpretation of figure 5 would be great. In general, the reader is a bit left alone with the interpretation of the figures. Either one understands it immediately on its own or not. Some help would be nice for all who didn't create the figures.

We regret any confusion regarding interpretation of this figure. The definitions of ramps are given in equation (3) and accompanying text in Methods. We have expanded that description this a little to read: 'The probability of wind speed and power production ramp events are computed from the NYSERDA and NYSM LiDARs and in the case of wind speeds are normalized as follows:

$$\frac{\delta u(t)}{\sigma_{\delta u}} = \frac{u(t+\tau) - u(t)}{\sigma_{\delta u}} \tag{3}$$

where *u(t)* is the wind speed at time *t*, *δu(t)* is the wind speed increment from the prior time step, *τ* is the chosen time increment, and $\sigma_{\delta u}$ is the standard deviation of the wind speed increments (DeMarco and Basu, 2018). $\frac{\delta u(t)}{\sigma_{\delta u}} = 2$ indicates an increase in wind speed between two consecutive measurements (here τ = 10 minutes) of a magnitude that is equal to two standard deviations of wind speed changes computed from the entire time series, and thus lies in highest 2.5% of values. Conversely, $\frac{\delta u(t)}{\sigma_{\delta u}} = -2$, has a similarly low probability but is associated with a large magnitude decline in wind speed between two consecutive measurements.'

We have also expanded the paragraph that links to Figure 5 to read:

'The second component of power quality is the intermittency in terms of the probability and magnitude of ramp events – that is rapid changes in wind speed and/or power production. Wind speed time series at 150 m height from the NYSM and NYSERDA LiDARs indicate clear similarities in terms of ramp event magnitude and frequency to those derived using data from the FINO1 platform in the North Sea, Cabauw onshore in western portion of the Netherlands, Høvsøre in coastal Jutland, Denmark, and NWTC in the foothills of the Colorado Rocky Mountains (DeMarco and Basu, 2018) (Figure 5). Data from the NYSERDA buoys indicate a low probability of wind speed ramps of all magnitudes relative to the NYSM LiDARs (Figure 5), and all LiDAR time series indicate a substantially higher probability of a ramp-up (increase) than a ramp-down (decrease) of a given magnitude in wind speeds. Wind speed ramps in hourly ERA5 data exhibit a narrower distribution owing to spatial and temporal averaging, illustrating the need for in-situ data for capturing high resolution wind variability (Figure 5). Consistent with the lower probability of large-magnitude rapid changes in wind speed offshore, data from the NYSERDA buoys (Hudson North E05 and Hudson South E06) indicate probabilities of a wind power ramp with > ±20% change in power are considerably lower than those from any of the onshore locations (Figure 5). Thus, the chance of experiencing an increase or decrease in electrical power production of 20% from one 10-minute period to the next is substantially lower for wind turbines deployed offshore. This indicates that wind turbines deployed offshore are likely to exhibit less intermittency in terms of electrical power production which is critical to efficient grid integration (Ayodele et al., 2012).'

We have also slightly modified the caption to Figure 5 to read:

'Figure 5. Left: probabilities of wind speed ramp events computed from the 10-minute data from the NYSERDA LiDAR buoys and the NYSM sites computed using Equation (3), and reported for four locations at or near operating wind turbines: FINO 1 is (offshore) in the North Sea, Cabauw is in the western portion of the Netherlands, Høvsøre is in Jutland, Denmark, and NWTC is in the foothills of the Colorado Rocky Mountains (data digitized from: (DeMarco and Basu, 2018)). Wind ramps computed from the hourly ERA5 output are shown by the gray polygon. Right: probabilities of wind power production ramp events at the locations of the NYSERDA buoys and the NYSM sites computed by applying the power curve for the IEA 15 MW reference wind turbine to the LiDAR wind speeds. The probabilities of no-change (i.e., power $\pm$ 0%) are not shown to aid visibility.'

Page 13, lines 304-305: Could you explain this a bit more, please. There is an image, you could lead the reader through the image, just a bit, and let someone not being such deep into statistics see the same like you. Furthermore, do you have an explanation/expectation why the e-folding times at sea are larger than on land and why there is a slight difference in the onshore stations? E.g., any physical reasons for that?

The reviewer is referring to the following: 'The third aspect of power quality is predictability. The autocorrelation in power production at different time lags for the NYSM LiDARs exhibit clear diurnal oscillations and shorter e-folding time scales.'

We hope that adding text in Introduction

'Predictability and persistence of wind speeds and power production (Haghi et al., 2013;Haslett and Raftery, 1989). Within liberalized electricity markets, wind farm owner/operators bid in advance (e.g. 24 hours in advance) and are charged penalties for any imbalance between the bid and actual production (Pinson et al., 2007). Hence, accurate forecasts of wind generation are important to reduce penalties and maximizing revenue (Barthelmie et al., 2008). Persistence models where the power production at some future time is model as a function of power production in the recent past is often used as a benchmark forecast against which more sophisticated short-term power production models are compared (Kariniotakis et al., 2004). Many statistical short-term forecast models are predicated in part on persistence (Zeng and Qiao, 2011) and thus are most skillful when the power production time series exhibits high temporal autocorrelation. We quantify the temporal autocorrelation of power production from each onshore and offshore site and compare the degree to which electrical power production from the onshore and offshore locations differ with respect to persistence and short-term predictability.'

And in the Methods to this sentence:

'Temporal autocorrelation coefficients of the power production time series are used to derive e-folding time scales (i.e. the time delay at which the correlation coefficient drops to e^{-1}, i.e. to 0.37) which is used to represent the time scale at which the system 'loses' the memory of the initial state (Wilks, 2011).'

And this where we discuss Figure 5:

'These relatively large e-folding times for the buoy locations indicate a longer atmospheric 'memory' at these sites, indicating the potential for more accurate short-term power prediction forecasts because each time step is strongly dependent on previous time step(s).'

Clarifies this matter.

Page 13, lines 308-309: Why does a large e-folding indicate the potential for more accurate power prediction? Are there any proofs? Did someone find this (citation?), or did you do any calculations?

Please see the answer directly above.

Page 15: What is the conclusion from the analysis of shear conditions and LLJ?
We have added these two sentences that we believe makes the inference more concrete:
'The implication is that large wind turbines deployed in these locations may experience a relatively high frequency of large unbalanced rotor loads and reduced component lifetimes unless such loads can be appropriately compensated (Hur et al., 2017).'
And
'It is important to acknowledge that comparisons of LLJ climates derived from LiDAR measurements and WRF modelling should be done cautiously and that LLJ detection from the LiDAR wind speed profiles is critically dependent on unbiased data availability. Nevertheless, this analysis suggests LLJ within the rotor plane, as a source of large unbalanced rotor loads and reduced blade lifetimes, are less frequent at these onshore locations. '
Page 15/16, chapter demand matching: How did you calculate the normalized demand and site WPP and how do you relate it to the demand? What does it exactly mean, which conclusions can you draw from the findings? I guess, the couple of positions equipped with one turbine per position will not be able to cover the energy demand, but from the image it looks a bit like this. Means: further explanations are needed here to guide the reader into the right direction. And what does the comparison with ERA-5 reveal?
We calculate the demand as follows (see Methods):
'Electrical demand (in MWh) for New York state are also presented and mean values are computed for each hour of the day and each month of the year based on hourly values for 2016-2022 as reported by the U.S. Energy Information Administration (EIA) hourly electric-grid monitor (https://www.eia.gov/electricity/gridmonitor/dashboard/electric_overview/US48/US48)'.
And we normalize it as noted in the caption to Figure 9: 'The data are normalized to a mean value of 1 and so that values of 0.9 or 1.1 in a given hour or month indicates WPP or demand that is 10% below or above the mean, respectively.'
We have expanded the paragraph that relates to Figure 9 to read as follows:
'Electricity demand in New York state tends to peak in the afternoon (~ 1700 eastern standard time, EST) and in summer (highest values in July), though a secondary maximum occurs in January (Figure 9). Wind power production calculated from the NYSM/NYSERDA LiDARs and ERA5 grid-cell data ($P150_{ERA5}$) show highest values at night (0100 to 0500 EST) and during winter to spring (December-April), with the lowest production during the day (1300 to 1600 EST) and during the summer (Figure 9). Wind power production estimated based on LiDAR data from the NYSERDA buoy locations exhibits markedly lower diurnal and seasonal variability than is estimated at the NYSM sites, varying by ± 10% around the mean versus ± 25% at NYSM. This results in a reduction in mean absolute error (MAE) between time series of normalized WPP from the offshore LiDAR and electricity demand on both diurnal and seasonal timescales. The MAE computed from the mean hourly offshore WPP and demand is 0.19 when computed over the 24 hours of the day (Figure 9a) and 0.13 when computed from the time series of monthly mean values (Figure 9b). Both are smaller than MAE computed from WPP from the onshore LiDARs and demand on these time scales which are 0.25 and 0.20, respectively. This implies there will be better matching to electricity demand for power production from wind turbines deployed offshore. '
We hope this clarifies.
Concluding remarks:
At best, I see a summary here but no conclusion and no answer to a concrete scientific question or proof of a hypothesis. The reader is more or less left alone with the interpretation of this statistical analyses.
We regret the reviewer found this section challenging to interpret. We have supplemented materials in the conclusions to help the reader. The conclusions now read:
'Comparative analyses of wind resources and projected power production quantity and quality at onshore and offshore locations have been hampered by the lack of high-quality hub-height wind speed

observations. Here we use uniquely detailed LiDAR measurements from an onshore profiler network and offshore campaign to compare projections of potential power generation quantity and quality from offshore and onshore locations in New York State (Figure 1). Returning to the study objectives articulated in section 1, the study results indicate there are significant benefits to offshore deployments of wind turbines:

- Wind resources at locations in the New York Bight (coastal offshore areas southeast of New York state, Figure 1) greatly exceed those of all onshore locations within New York state. The mean wind speeds at 150 m ($\overline{U}$) offshore are above 10 ms^{-1}, while $\overline{U}$ is below 8 ms^{-1} at all onshore sites. Weibull distribution fits to the 10-minute wind speed time series indicate scale parameters that are higher by 2 ms^{-1} than all onshore locations (Figure 4) except EHAM which is on Long Island and is within 1 km of the coastline (Figure 1). Accordingly, energy densities are 40% higher offshore and power production estimated offshore using the power curve of the IEA 15 MW wind turbine (Figure 2) yield over twice the AEP estimated for all onshore sites except EHAM (Table 2). Power generation estimated from wind speed time series offshore also exhibits lower variability on diurnal and seasonal time scales (Figure 6) and improved matching to current electricity demand in New York State (Figure 9). This implies that not only is the offshore resource considerably larger offshore, but the ability to meet electricity demand is better for wind turbines deployed offshore.
- Analyses presented herein also suggest that power generation intermittency is lower for the offshore sites. The probability of wind speeds below cut-in or above cut-out for the IEA reference wind turbine is lower offshore, as is the probability of large magnitude wind speed and power ramps (Figure 5). For example, the probabilities of wind power ramps with > ±20% change in power over a 10-minute period are less than half as probable offshore as onshore. The higher temporal autocorrelation of wind power production offshore (Figure 6 and Table 2) may also aid the accuracy of short-term wind power forecasting for wind turbines deployed offshore, yielding economic benefits to wind farm owner/operators and enabling grid integration.

Conversely, the frequency of anomalous wind speed shear and LLJ close to, or within, the rotor plane computed from the NYSM LiDAR wind speed profiles are slightly higher than those previously reported for the offshore areas from numerical simulations (Aird et al., 2022) but LLJ also exhibit higher elevations of the jet cores (Figure 8) and thus may be of less concern to wind turbine loading.

An analysis of the distance dependence of the co-variability of power production derived from measured 10-minute mean wind speed time series at the onshore and offshore sites indicates that the non-parametric Spearman correlation coefficient drops below 0.4 at distances of about 350 km (Figure 7). This indicates that in order to ensure consistency of electrical power production from wind farms in New York state, major developments should be separated by more than 350 km. This information could be used to guide judicious selection of wind farm locations to minimize the probability of concurrent low generation from onshore and offshore sites.

Thus, in accord with a priori expectations, analyses presented herein indicate there are advantages to the emerging trend towards offshore wind energy deployments in terms of the wind resource and the expected power quality and predictability (reduced ramp events, higher probability of rated power, etc.). Despite higher project AEP for the offshore locations, the additional costs involved in installing and operating offshore wind farms results in higher LCoE estimates for the offshore sites (Table 2). LCoE estimates derived using AEP at the NYSM sites are 26 to 49 \$/MWh while estimates for the NYSERDA buoy locations are 62-64 \$/MWh. Nevertheless, projected LCoE from wind energy for all of the sites investigated here in NY are competitive with all other electricity generation sources, with the possible exception of utility-scale PV, and much less expensive than traditional sources such as coal and nuclear that, according to a recent analysis, have an unsubsidized LCoE of 65-152 \$/MWh and 131-204 \$/MWh, respectively (Lazard, 2023).'

Page 16, lines 386-387: You compare the data to find out what? For what is it helpful, what does it aim for?
We hope the rewrite of the introduction and conclusion helps – we are seeking to quantify the relative benefits of deploying wind turbines offshore.
Page 17: 402-403: This is only a guess, I didn't see neither a proof nor a clear or understandable assessment of this (as has been stated in the introduction).
No its not a guess the statement "higher temporal autocorrelation of wind power production offshore (Figure 6 and Table 2) may also aid the accuracy of short-term wind power forecasting" can be readily made because virtually all statistical short-term forecasting methods employ directly or indirectly methods that are predicated on red noise characteristics of the atmosphere. See additional text that explains that matter.
Page 17, line 410-411: To what extent does this follow from the Spearman correlation coefficients drop?
Exponential decay of atmospheric properties in time and space is well documented. We hope that explanatory text we have added about this matter helps.
Page 17, line 414-420: The LCoE and its calculation was not mentioned in the results.
We have moved some discussion of LCoE into section 4.1
Figures:
Figure 3: For the comparison between onshore and offshore wind speeds I would suggest to create the same ranges for the y-axes. Also, the onshore figure is a bit crowded, maybe it would be a bit clearer to put the data availability into an own subfigure.
We do not concur with the reviewer. We think there is importance to having the reader readily be able to note the data availability with the monthly mean wind speeds.
Figure 5: The figure is quite crowded, very small and differences are hard to interpret. I would also love to see a much better description in the text.
We have elaborated the text as requested.
Figure 6: The lag time is in 10 Minute intervals, which needs an ad hoc recalculation to hours while reading the text, which in turn states the e-folding times in hours. I would recommend adapting either the text or, even better, the figures x-axis in a way that both becomes consistent.
Text changes enacted as requested.
Figure 8: Again very crowded, again, the image is not intuitively understandable without a more detailed description in the text.
We regret the reviewer struggled to understand this figure. We have added this text to the caption:
'A LLJ frequency of 5% calculated from the LiDAR deployed at QUEE for the calendar month of May indicates that LLJ were indicated in 5% of all 10-minute periods during this month. Data in panels (a) and (b) indicate that at that site in the month of May the associated LLJ mean core wind speed is 11 ms^{-1} and the mean core height above ground is 330 m.'

Reviewer #2:

General comments:

The paper presents data from a set of onshore and offshore lidars. The paper mostly presents statistics based on these data and the results of the analysis are as expected, as the wind blows more and more steady offshore compared to onshore. There is no new methods, concepts or ideas introduced in the manuscript, so I have rated the scientific significance as low. Nonetheless, the paper could be useful for somebody that is looking specifically for information about the wind climate in this region.
We regret the reviewer did not find the scientific significance to be higher. The lack of measurements at

wind turbine hub-heights and above has long been a source of concern for the wind energy community so we believe that the availability of network based LIDAR data will be of general interest. Further, we have found no previous research that used these types of data sets to quantitatively compare; the resource, power quality, demand matching etc on – and offshore in the same climate zone. And yet these properties are of critical importance in charting the future of wind energy deployments.

My main comment on the analysis itself is about the low data recovery percentage of the lidar data. It is not demonstrated that there is no correlation of when data recovery is low and what the wind climate is. For example, one would expect that the lidars return 'not available' when a measurement cannot be obtained. Most of these data will be during low wind speed conditions when there is not enough aerosols to measure the wind. You have your long-term measurement time series from ERA5, so you could correct for this. Also in general I miss some discussion of the type of lidars you are using, because they are not the same offshore (zephyr) and onshore (windcube). What kind of filtering was done (precipitation? CNR?).

It is indeed regrettable that the NYSM network does not have higher data recovery. We asked this question of the operators of the NYSM but they are not able to provide further information beyond what is available via the readme documentation (available at: http://www.nysmesonet.org/networks/profiler#stid=prof_alba) which simply states: 'Sensor and/or system failures are not uncommon as the Profiler equipment are sensitive to a variety of environmental factors. Data gaps may be due to sensor failures; calibration errors; power failures; and/or communication failures. … Only manufacturer-developed QA/QC procedures are applied to the data and there might still be some undetected errors.'

More information is available regarding the NYSERDA buoy deployments – e.g. via technical reports available for download from: https://oswbuoysny.resourcepanorama.dnv.com/download/f67d14ad-07ab-4652-16d2-08d71f257da1

We have added a note to that effect to the Data availability statement: 'Reports documenting LiDAR performance verification are also available for download from: https://oswbuoysny.resourcepanorama.dnv.com/download/f67d14ad-07ab-4652-16d2-08d71f257da1.'

Regarding the comment 'It is not demonstrated that there is no correlation of when data recovery is low and what the wind climate is.' We think there are two concepts of importance here:

1) We do document at the monthly scale data availability versus wind speed.
2) There is no documented evidence from NYSM that the LiDAR scans failed to report wind speeds due to low aerosol concentrations but given they state 'manufacturers QA/QC procedures were employed it is highly likely a CNR screen was employed'. That having been said air quality measurements in New York state DO NOT imply a high frequency of sufficiently low aerosol concentrations to render these LiDARs likely to be unable to operate (see for example; Squizzato, S., Masiol, M., Rich, D. Q., & Hopke, P. K. (2018). A long-term source apportionment of PM2. 5 in New York State during 2005–2016. *Atmospheric Environment*, *192*, 35-47.)

We have added this text to section 4.1; 'Documentation associated with the data set notes the causes as; 'calibration errors; power failures; and/or communication failures.' And further notes 'Only manufacturer-developed QA/QC procedures are applied to the data and there might still be some undetected errors.' (readme accessible from http://www.nysmesonet.org/networks/profiler#stid=prof_alba).'

Technical comments:

l13: factor -> parameter

Done.

l166: conventional usage would be capital gamma changed as requested.

l211-215: since the lidar signal depends on aerosol concentration this method will likely miss many low-level jets as the lidar will simply not return a signal above the jet. Would be good to discuss this.

We have added this cautionary text:

'It is important to acknowledge that comparisons of LLJ climates derived from LiDAR measurements and WRF modelling should be done cautiously and that LLJ detection from the LiDAR wind speed profiles is critically dependent on unbiased data availability. Nevertheless, this analysis suggests LLJ within the rotor plane, as a source of large unbalanced rotor loads and reduced blade lifetimes, are less frequent at these onshore locations.'

In addition: I am not quite sure how to interpret the comment about the comparibility with the 500 m height: did you use data up to 500 m? It would be good to show what the recovery percentage is at this height, related to the remark above.

We have calculated the data recovery rates at each LiDAR location at each height < 500 m and now report them, see text that's reads; 'Analyses of wind speed data from the NYSM LiDARs at all measurement heights from 100 to 500 m indicates that averaged across all stations the data availability as a function of height varies only by +/-2.5%.'

l232: move bracket from before Barthelmie to before 2023.

Done.

Quantitative Comparison of Power Production and Power Quality Onshore and Offshore: A Case Study from the Eastern U.S.

~~Onshore and Offshore Wind Resources and Operating Conditions in the Eastern U.S.~~

Rebecca Foody[1], Jacob Coburn[1], Jeanie A. Aird[2], Rebecca J. Barthelmie[2] and Sara C. Pryor[1]

[1]Department of Earth and Atmospheric Science, Cornell University, Ithaca, 14850, United States
[2]Sibley School of Mechanical and Aerospace Engineering, Cornell University, Ithaca, 14850, United States

Correspondence to: Sara C. Pryor (sp2279@cornell.edu)

Abstract. A major issue in quantifying potential power generation from prospective wind energy sites is the lack of observations from heights relevant to modern wind turbines, particularly for offshore where blade tip heights are projected to increase beyond 250 m. We present analyses of uniquely detailed datasets from LiDAR (Light Detection And Ranging) deployments in New York s~~S~~tate and on two buoys in the adjacent New York bight to examine the relative power generation potential and power quality at these on- and off- shore locations. Given the relatively close proximity of these LiDAR deployments, they share a common synoptic scale meteorology and seasonal variability with lowest wind speeds in July and August. Time series of power production from the on- and off- shore location are highly spatially correlated with the Spearman rank correlation coefficient dropping below 0.4 for separation distances of approximately 350 km. Hence careful planning of on- and off- shore wind farms (i.e. separation of major plants by > 350 km) can be used reduce the system-wide probability of low wind energy power production. ~~Time series of 10-minute wind power production are computed from these wind speeds using the power curve from the International Energy Agency 15 MW reference wind turbine.~~ Energy density at 150 m height at the offshore buoys is more than 40% higher and the Weibull scale ~~factor~~ parameter is 2 ms^{-1} higher than at all but one of the land sites. ~~Given the relatively close proximity of these LiDAR deployments, they share a common synoptic scale meteorology and hence the~~exhibit ~~seasonal variability of wind speeds~~trends ~~is similar with lower wind speeds in July and August. Accordingly, time series of power production from the on- and off- shore location are highly spatially correlated with the Spearman rank correlation coefficient dropping below 0.4 for separation distances of approximately 350 km~~. Hence~~, but careful planning of on- and off- shore wind farms can reduce the system-wide probability of lower wind energy power production.~~ Time series of 10-minute wind power production are computed from these wind speeds using the power curve from the International Energy Agency 15 MW reference wind turbine. Analyses of the resulting power production time series indicate ~~AEP~~ Annual Energy production is almost double for the two offshore locations. Further, electrical power production quality is higher from the offshore sites that exhibit a lower amplitude of diurnal variability, plus a lower probability of wind speeds below the cut-in and of ramp events of any magnitude. Despite this and the higher resource, the estimated Levelized Cost of Energy (LCoE) is higher from the offshore sites mainly due to the higher infrastructure costs. Nonetheless, the projected LCoE is highly competitive from all sites considered.

1 Introduction

The United States government has set a goal of reaching carbon net neutral emissions from the power generation sector by 2035 and a carbon net neutral economy by 2050 (U.S. White House, 2023). As part of this plan, the U.S. Department of Interior is committed to deploying 30 GW of offshore wind power by 2030 (U.S. Department of the Interior, 2021). However, in 2021, 93% of electrical power produced by global wind turbines was derived from those deployed in onshore rather than offshore wind farms, partly due to the higher investment required for offshore wind power installation (IEA, 2022). Within the U.S., as of the end of 2022, there was over 145 GW of wind energy installed capacity onshore and only 42 MW offshore (American Clean Power, 2023).

Enhanced deployment of wind turbines offshore offers great promise in terms of enhanced renewable energy penetration into the electricity generation portfolio for three primary reasons:

- First, wind speeds tend to be higher and more consistent offshore due to both the lower surface roughness and lack of obstacles and topographic features that extract momentum and reduce both the wind speed and wind resource (Pryor and Barthelmie, 2002). Accordingly, Capacity Factors (CF), which are the ratio of actual annual power generation divided by the theoretical maximum power generation, are typically higher offshore. For example, ~~D~~data from operating wind farms in Denmark indicate CF from four offshore wind farms with installed capacity (IC) of 160 to 400 MW of 41-53% while CF from smaller onshore wind farms (IC: 16-70 MW) have CF of 28-41% (Enevoldsen and Jacobson, 2021). Within the U.S., the mean CF for onshore wind farms built between 2014 and 2019 is approximately 41% (Wiser et al., 2021). Simulations using numerical models for offshore wind energy lease areas along the U.S. east coast indicate CF above 46% largely as a result of the higher wind speeds offshore (Pryor et al., 2021;Barthelmie et al., 2023).
- Second, there are fewer social barriers than exist on land (e.g., competition for land, noise concerns, visual blight, etc.) (Diógenes et al., 2020) and onshore resource in available areas may not be sufficient to meet projected needs (Esteban et al., 2011). In this context it is worth noting that the U.S. technical offshore wind capacity exceeds 2000 GW with the potential to produce over 7200 TWh per year, nearly twice current U.S. electricity use (4240 TWh) (Musial et al., 2016).
- Third, many major metropolitan areas are located near coastlines, making offshore wind a convenient energy source (Pryor et al., 2021). The cost of transmission and electricity loss during transmission across high-voltage lines both increase with transportation distance (Bamigbola et al., 2014).

Here we focus on the first of these reasons, and specifically seek to quantify the potential benefit of offshore wind turbine deployments using analyses of uniquely detailed wind profiles from an onshore LiDAR (Light Detection And Ranging) network and an offshore LiDAR network. ~~Relatively few previous studies have directly compared onshore and offshore wind climates at heights of relevance to modern wind turbines and in terms of electrical power generation quantity and quality. This is in part due to the very low availability of measured wind speed profiles at those heights. Here we employ long term (multi-year) measurements from two major LiDAR (Light Detection And Ranging) field deployments: the New York State Mesonet (NYSM) onshore LiDAR network and the New York State Energy Research and Development Authority (NYSERDA) floating LiDAR campaign.~~ ~~All of the locations considered here lie within a separation distance of a few hundred kilometers and hence are within the so-called 'macro-beta' scale that is influenced by synoptic scale transitory mid-latitude cyclones (i.e., 400-4,000 km) (Stull, 2017). Thus, the expectation is that all sites will experience a relatively similar synoptic scale meteorological regime.~~ We use these data sets to quantify and compare ~~evaluate four~~ three aspects of the wind power generation potential on- and offshore:

1. ~~Assessment of~~Wind resource and power production~~ potential~~. ~~Here w~~We present Weibull probability distribution parameters and derive energy density from the wind speed time series and compare and contrast the inferred wind resource at the onshore and offshore sites. We further compute and compare the Annual Energy Production (AEP) from the time series of wind speeds at each LiDAR site using a common wind turbine power curve.
2. P~~Assessment of p~~ower quality. Intermittency is frequently cited as a barrier to increased wind power integration into the electrical grid (Bistline and Blanford, 2021). We quantify and compare the frequency ~~and intensity~~ of zero power production and ~~the~~ intensity and probability of so-called ramp events (i.e., rapid changes in wind speed and power

production) (DeMarco and Basu, 2018;Pichault et al., 2021) from each onshore and offshore site where ~~the~~ LiDARs have been deployed.

3 P~~Assessment of p~~redictability and persistence of wind speeds and power production (Haghi et al., 2013;Haslett and Raftery, 1989). Within liberalized electricity markets, wind farm owner/operators bid in advance (e.g. 24 hours in advance) and are charged penalties for any imbalance between the bid and actual production (Pinson et al., 2007). Hence, accurate forecasts of wind generation are important to reduce penalties and maximize revenue (Barthelmie et al., 2008). Persistence models where the power production at some future time is modeled as a function of power production in the recent past is often used as a benchmark forecast against which more sophisticated short-term power production models are compared (Kariniotakis et al., 2004). Also many statistical short-term forecast models are predicated in part on persistence (Zeng and Qiao, 2011) and thus are most skillful when the power production time series exhibits high temporal autocorrelation. We quantify the temporal autocorrelation of power production from each onshore and offshore site and compare the degree to which electrical power production from the onshore and offshore locations differ with respect to persistence and short-term predictability.

We further use these LiDAR measurements to quantify and compare a key driver of wind turbine loading at the on- and off-shore locations:

4 Extreme or ~~anonymous~~anomalous wind shear across the rotor plane. Low-Level Jets (LLJ) are confined wind speed maxima within the lower atmospheric boundary layer (Stensrud, 1996) and ~~, LLJ~~ are associated with enhanced vertical wind speed (and sometimes directional) shear relative to typical near-logarithmic profiles. LLJ ~~and thus~~ within the wind turbine rotor plane are associated with higher aerodynamic and structural loading (Gutierrez et al., 2019;Gadde et al., 2021)~~ and can modify wind turbine wake propagation (Gadde and Stevens, 2021)~~. Analyses of simulations with the Weather Research and Forecasting (WRF) model suggest that offshore coastal regions of the U.S. mid-Atlantic (including the locations of the buoys from which data are presented) generally exhibit a weakly sheared profile across the rotor plane and a relatively low frequency of LLJ (Aird et al., 2022). That analysis found LLJ in the lowest 500 m of the atmosphere are most frequent south of Massachusetts and during the summer (8% of all hours). They frequently occur at heights that intersect the wind turbine rotor plane, and at wind speeds within typical wind turbine operating ranges. Further, LLJ diagnosed from the WRF output were most intense and have lowest elevation under strong horizontal temperature gradients and lower planetary boundary layer heights. For comparative purposes, data from the NYSM LiDARs are used here to evaluate wind shear across the rotor plane and the occurrence, intensity, and height of LLJ at the onshore locations.

~~3~~ We also analyze the LiDAR data to quantify two other properties of relevance to wind energy integration into the electricity generation supply:

~~4~~5 ~~Assessment of the degree of c~~Co-variation of wind speeds and power production with varying distance separation (Pryor et al., 2014;Solbrekke et al., 2020). The electric power transmission network in the contiguous U.S. comprises three main interconnections (eastern, western, and Electric Reliability Council of Texas (ERCOT)) and 66 'balancing authorities' that oversee regional operation of the electric grid and are referred to as Regional Transmission Operators (RTOs) or Independent System Operators (ISOs). New York (NY) state currently operates as a single state ISO. NY is both a net importer of electricity and the third most efficient state in terms of energy use per U.S. dollar of economic activity (https://www.eia.gov/state/analysis.php?sid=NY). Careful planning of wind farm locations on and offshore could ~~will~~ ensure stable supply of wind-generated electricity into the grid and thus aid the transition from electricity imports and a current dependence on nuclear and natural gas ~~by ensuring stable supply of wind-generated electricity~~ (Eryilmaz et al., 2020). Here we quantify the spatial autocorrelation of power production from each onshore and offshore site where the LiDARs have been deployed to evaluate the decorrelation distance and hence provide guidance regarding optimal spatial scale of wind farm separation (on- and off-shore) for stability of wind power supply.

~~Although the LiDAR data sets that we analyze here are – to our knowledge – unique in terms of the duration and number of sites considered, we also contextualize the results and inferences drawn from these multi-year, but relatively short duration, observations using the > 40 year duration ERA5 reanalysis product (Hersbach et al., 2020).~~

~~Low-Level Jets (LLJ) are confined wind speed maxima within the lower atmospheric boundary layer (Stensrud, 1996). LLJ are associated with enhanced vertical wind speed (and sometimes directional) shear relative to typical near-logarithmic profiles and thus are associated with higher aerodynamic and structural loading (Gutierrez et al., 2019;Gadde et al., 2021) and can modify wind turbine wake propagation (Gadde and Stevens, 2021). Analyses of simulations with the Weather Research and Forecasting (WRF) model suggest that offshore coastal regions of the U.S. mid-Atlantic (including the locations of the buoys from which data are presented) generally exhibit a weakly sheared profile across the rotor plane and a relatively low frequency of LLJ (Aird et al., 2022). That analysis found LLJ in the lowest 500 m of the atmosphere are most frequent south of Massachusetts and during the summer (8% of all hours). They frequently occur at heights that intersect the wind turbine rotor plane, and at wind speeds within typical wind turbine operating ranges. Further, LLJ diagnosed from the WRF output were most intense and have lowest elevation under strong horizontal temperature gradients and lower planetary boundary layer heights. For comparative purposes, data from the NYSM LiDARs are used here to evaluate wind shear across the rotor plane and the occurrence, intensity, and height of LLJ.~~

6 Seasonality and diurnal variability of wind power production (WPP) on- and off-shore for demand matching.

Electricity demand varies with the level of economic activity and seasonal heating/cooling requirements which are a function of the regional climate (Castillo et al., 2022;Staffell and Pfenninger, 2018). Generally, electricity demand in the U.S. is minimized between approximately 0400 and 0600 local time (LT), is high between 0800 and 1600 LT, and peaks between 1800 and 2100 LT (Burleyson et al., 2021). Diurnal variability of wind power generation is a function of location and land use but, for example, in ERCOT is highest at night (Kiviluoma et al., 2016), consistent with the expectation based on day-time variations in atmospheric stability caused by changes in net radiation and the surface energy balance. Because the oceans have higher specific heat capacity than land, this scale of variability is typically not present in the far offshore (> 20 km from the coast) (Barthelmie et al., 1996). At the seasonal scale, wind resources and power production in the midlatitudes and specifically the contiguous U.S. tend to peak in between October and April and are lowest in July or August due to pronounced shifts in the storm track and the frequency and intensity of mid-latitude cyclones (Pryor et al., 2020b). Recent research suggests ~~it~~ WPP is highest in southeastern Canada and the northeastern U.S. during January and February (Coburn and Pryor, 2023). Thus, finally, we ~~consider~~ quantify whether electrical power from wind turbines deployed offshore exhibit higher or lower temporal matching with electricity demand in New York state at both the diurnal and seasonal scales.

2 Data sources

~~2~~ Here we analyze long term (multi-year) measurements from two major LiDAR (Light Detection And Ranging) field deployments: the New York State Mesonet (NYSM) onshore LiDAR network and the New York State Energy Research and Development Authority (NYSERDA) floating LiDAR campaign. All of the locations considered here lie within a separation distance of a few hundred kilometers and hence are within the so-called 'macro-beta' scale that is influenced by synoptic scale transitory mid-latitude cyclones (i.e., 400-4,000 km) (Stull, 2017). Thus, the expectation is that all sites will experience a relatively similar synoptic scale meteorological regime and that differences in wind resources, power quality and so forth can be largely attributed to differences in the surface; land versus ocean.

2.1 NYSERDA LiDAR buoys

To support development of offshore wind energy, NYSERDA undertook a campaign to deploy LiDAR on buoys near prospective offshore wind lease areas (Optis et al., 2021). Here we present data from two of those locations (Figure 1): the Hudson North E05 buoy is located within the Ocean Winds East (OCS-A 0537) lease area, and the Hudson South E06 buoy is located along the Bight Wind Holdings (OCS-A 0539) lease area (BOEM, 2023). The LiDARs deployed on these buoys are ZephIR ZX300M units. They report mean wind speeds, wind direction, and other properties in 10-minute intervals every 20 m up to a maximum height of 200 m. The performance of different series of these robust LiDARs have been extensively evaluated (Barthelmie et al., 2016;Kelberlau and Mann, 2022;Smith et al., 2006) and best practice has been developed for deployment of LiDARs on floating platforms (Bischoff et al., 2017). The LiDAR from the Hudson North E05 buoy has data available from August 2019 through February 2022. The LiDAR on the Hudson South E06 buoy operated from September 2019 through February 2022 but there is lower data availability during August through November (which is partly due to a temporary break in data collection for repairs to the buoy). The LiDARs have an overall data recovery rate of wind speeds at approximately ~~145~~ 140 m above sea level of about 77% for the Hudson North E05 buoy and 67% for the Hudson South E06 buoy.

2.2 New York State Mesonet

New York state has also invested in a Mesonet (NYSM) to aid hazard mitigation and disaster preparedness. The NYSM includes a network of 17 profiler stations (Shrestha et al., 2022;Brotzge et al., 2020). The LiDARs deployed as part of the NYSM are the Leosphere WindCube WLS-100 series Doppler LiDAR (Bingöl et al., 2010;Kumer et al., 2016). These pulsed LiDARs have a vertical range of many kilometers and are also configured to report wind speed and direction measurements every 25 m in 10-minute intervals. The period for which data are available varies by location but is generally from January 2019 to December 2022. The sites listed in alphabetical order with their respective abbreviation and in terms of data availability for wind speeds at 150 m are: Albany (ALBA, 36.7%), Belleville (BELL, 29.8%), Bronx (BRON, 64%), Buffalo (BUFF, 44.0%), Chazy (CHAZ, 53.3%), Clymer (CLYM, 48.4%), East Hampton (EHAM, 68%), Jordan (JORD, 51.6%), Owego (OWEG, 56%), Queens (QUEE, 73%), Red Hook (REDH, 54.8%), Staten Island (STAT, 57%), Stonybrook (STON, 59%), Suffern (SUFF, 36.2%), Tupper Lake (TUPP, 53.6%), Wantagh (WANT, 62%), and Webster (WEBS, 49.3%). For much of the following analyses, only the seven sites with data recovery rates (i.e., wind speeds available at 150 m height) > 55% are included.

As indicated by the above, all LiDAR data time series are incomplete and the NYSM data sets are particularly biased toward data availability in the summer months. Thus, in the following additional analyses are performed for the 'best available year', defined as the 365-day period that has highest data availability computed across both NYSERDA buoys and the seven NYSM sites. This 'best year' extends from September 19, 2019, at 22:50:00 EST to September 18, 2020, at 22:50:00 EST. Data availability in each of the nine sites for this period is: BRON (67.0%), EHAM (72.9%), OWEG (69.4%), QUEE (78.7%), STAT (60.0%), STON (70.1%), WANT (79.3%), Hudson North E05 (92.1%), and Hudson South E06 (86.6%).

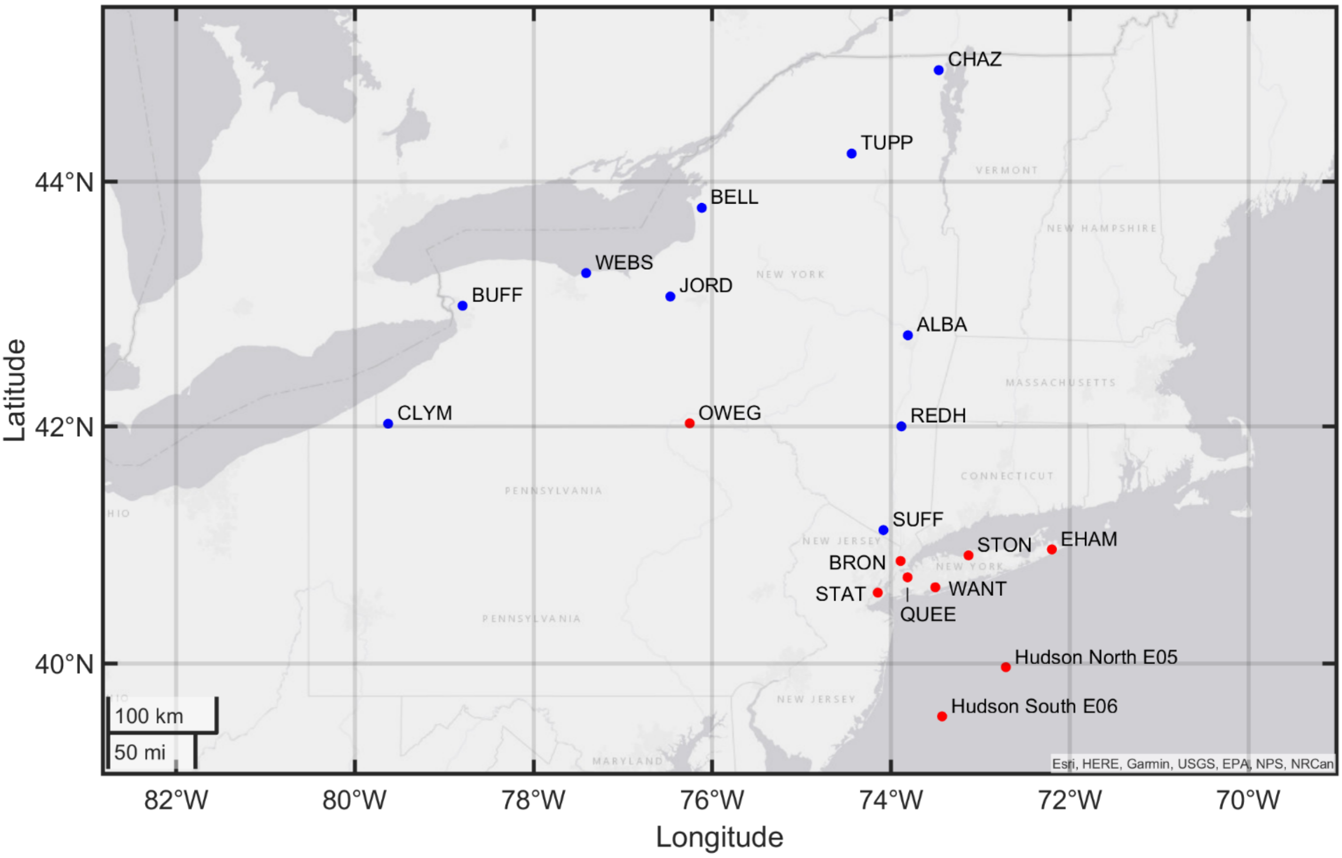

Figure 1. Map of the locations of the two NYSERDA LiDAR buoys and the 17 NYSM stations. Red points indicate the buoys and seven NYSM sites with the highest data recovery; blue points indicate the remaining NYSM sites.~~All of the locations considered here lie within a separation distance of a few hundred kilometers and hence are within the so-called 'macro-beta' scale that is influenced by synoptic scale transitory mid-latitude cyclones (i.e., 400-4,000 km) (Stull, 2017). Thus, the expectation is that all sites will experience a relatively similar synoptic scale meteorological regime.~~

2.3 ERA5 reanalysis

Wind data from the European Centre for Medium-range Weather Forecasting ERA5 reanalysis is used to provide a climatological context for analyses of the LiDAR data. Although the LiDAR data sets that we analyze here are – to our knowledge – unique in terms of the duration and number of sites considered, we also contextualize the results and inferences drawn from these multi-year, but relatively short duration, observations using the > 40 year duration ERA5 reanalysis product (Hersbach et al., 2020). This analysis explicitly acknowledges the presence of low-frequency variability (seasonal to multi-decadal) in mid-latitude wind speeds and wind resources (Pryor et al., 2020a) and is designed to quantify the uncertainty on mean wind speeds and power production computed from the relatively short LiDAR data time series.

The ERA5 reanalysis system assimilates a broad range of observing station, buoy, radiosonde, and satellite data and many atmospheric variables including wind components are available at an hourly time step with a spatial resolution of 0.28° × 0.28° (Hersbach et al., 2020). Here we use output of the u- and v- wind components at 100 m reported at an hourly disjunct frequency and that represent approximately 15- to 20-minute average values for the period of record with highest quality data assimilated into the reanalysis system: 1979-2022. This interval also includes the observational period of the LiDARs. ERA5 estimates of wind and wave conditions has been extensively independently evaluated and shown to exhibit relatively high fidelity (Pryor et al., 2020b;Gramcianinov et al., 2020;Sharmar and Markina, 2020;Hallgren et al., 2020).

2.4 Electricity demand

Electrical demand (in MWh) for New York state are also presented and mean values are computed for each hour of the day and each month of the year based on hourly values for 2016-2022 as reported by the U.S. Energy Information Administration (EIA) hourly electric-grid monitor (https://www.eia.gov/electricity/gridmonitor/dashboard/electric_overview/US48/US48).

3 Methods

3.1 Wind resource and potential power production

Two-parameter Weibull distributions (A = scale and k = shape) are fitted using maximum likelihood estimation (Pryor et al., 2004) and used to describe the probability distributions of wind speeds (U) at/close to 150 m height from each LiDAR:

$$f(U) = \frac{k}{A} \cdot (\frac{U}{A})^{k-1} \cdot exp(-(\frac{U}{A})^{k}) \tag{1}$$

The power in the wind that can be harnessed by wind turbines is often described using the energy density which can be derived from the time series of wind speed measurements or the Weibull distribution parameters:

$$E = \frac{1}{n} \cdot \frac{1}{2} \cdot \rho \cdot \sum_{1}^{n} U^{3} = \frac{1}{2} \cdot \rho \cdot A^{3} \cdot \cancel{\gamma}\Gamma(1 + \frac{3}{k}) \tag{2}$$

where E is in Wm^{-2}, ρ is the air density, and n is the number of time stamps from which wind speeds are available and $\Gamma\cancel{\gamma}$ is the gamma function (Troen and Lundtang Petersen, 1989).

The electrical power that would be generated by a wind turbine located at each LiDAR site is determined using the power curve from the International Energy Agency (IEA) 15 MW reference wind turbine which has a hub-height of 150 m and a rotor diameter of 240 m (Figure 2). We acknowledge that the physical dimensions and rated capacity of wind turbines deployed offshore are much larger than those that have traditionally been deployed onshore, but use of a single wind turbine allows direct comparison across sites. The time series of 10-minute power production and Annual Energy Production (AEP, in MWh/yr), i.e., the sum of the electrical power production in a year from a single 15 MW wind turbine at each LiDAR location, are used herein for the estimation of electrical power production and power quality.

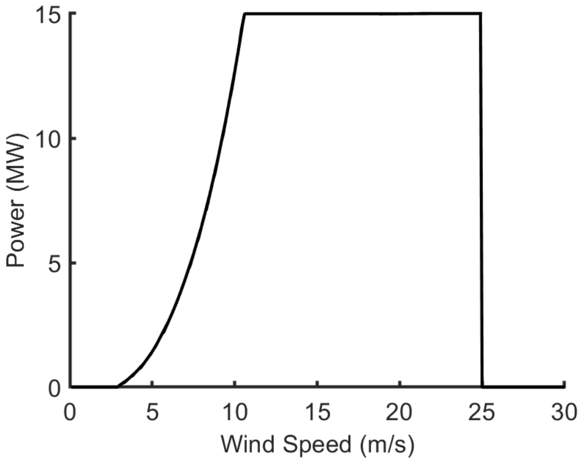

Figure 2. Power curve for the IEA 15 MW reference wind turbine (Gaertner et al., 2020).

3.2 Power quality

The probability of wind speed and power production ramp events are computed from the NYSERDA and NYSM LiDARs and in the case of wind speeds are normalized as follows:

$$\frac{\delta u(t)}{\sigma_{\delta u}} = \frac{u(t+\tau) - u(t)}{\sigma_{\delta u}} \tag{3}$$

where $u(t)$ is the wind speed at time t, $\delta u(t)$ is the wind speed increment from the prior time step, τ is the chosen time increment, and $\sigma_{\delta u}$ is the standard deviation of the wind speed increments (DeMarco and Basu, 2018). $\frac{\delta u(t)}{\sigma_{\delta u}} = 2$ indicates an increase in wind speed between two consecutive measurements (here τ = 10 minutes) of a magnitude that is equal to two standard deviations of wind speed changes computed from the entire time series, and thus lies in highest

2.5% of values. Conversely, $\frac{\delta u(t)}{\sigma_{\delta u}} = -2$, has a similarly low probability but is associated with a large magnitude decline in wind speed between two consecutive measurements.

Spatial and temporal correlation coefficients are also presented herein. In all cases, non-parametric Spearman rank correlation coefficients are used because wind speeds and power production are not Gaussian distributed variables (Wilks, 2011). Temporal autocorrelation coefficients of the power production time series are used to derive e-folding time scales (i.e. the time delay at which the correlation coefficient drops to e^{-1}, i.e. ~ ~~to~~ 0.37) which is used to represent the time scale at which the system 'loses' the memory of the initial state (Wilks, 2011). To assess the statistical significance of the correlation coefficients, a student's t-test is used (Wilks, 2011). In this process, a t-statistic is computed from the correlation coefficient (r) and the sample size (n):

$$t = r \cdot \sqrt{\left(\frac{n-2}{1-r^2}\right)} \tag{4}$$

Due to the high correlation in time, n is corrected to the effective sample size (n') using:

$$n' \approx n \cdot \frac{1-r_1}{1+r_1} \tag{5}$$

where r_1 is the lag 1 autocorrelation and n is the total number of samples. The resulting t-score is compared with critical values (t_{crit}) for n'. If $t > t_{crit}$, the correlation coefficient is statistically different from zero for a confidence level of 99% and the wind speed time series or electrical power production time series from two sites are significantly correlated.

Spatial correlation coefficients are also computed for power production time series from the onshore and offshore sites to examine the association as a function of separation distance and thus the degree to which power production across sites will be synchronized in time. The e-folding concept can also be applied in this context, to quantify the distance at which the power production from two sites is no longer significantly correlated. Past research has generally found that the correlation between wind speeds and wind power production from wind farms exhibits an exponential decay with increasing separation distance (St. Martin et al., 2015). Herein we fit both single exponential and double exponential fits with the forms:

$$y = a \cdot \exp(b \cdot x) \tag{6a}$$

$$y = a \cdot \exp(b \cdot x) + c \cdot \exp(d \cdot x) \tag{6b}$$

where y is the Spearman correlation coefficients for the time series of 10-minute power production estimated at the NYSERDA and NYSM sites, and x is the spherical separation distance between those locations. Fit coefficients; a, b, c and d are derived using maximum likelihood estimation (Wilks, 2011).

3.3 Wind profiles

To quantify the wind shear across the rotor plane we invoke the power law:

$$\frac{U_1}{U_2} = \left(\frac{z_1}{z_2}\right)^{\alpha} \tag{7}$$

where U_x is the wind speed at height (z_x) and α is the shear coefficient f(stability, surface roughness length) (Irwin, 1979). The International Electrotechnical Commission (IEC) 61400-1 standard states the expected value of α over land is 0.2 and is typically in the range of 0.05 to 0.25 and uses a value of 0.2 in the normal wind profile model (IEC, 2019). The occurrence of α beyond this range implies shear across the rotor plane differs from this design expectation and hence may indicate higher mechanical loading. Profiles of wind speeds from the NYSM LiDARs are used with equation (7) to quantify the frequency of occurrence of anomalous shear in two classes; negative shear exponents and $\alpha > 0.3$ conditionally sampled to include only periods when the 150 m wind speed is above 3 ms^{-1}, the cut-in for the IEA 15 MW reference wind turbine. Due to the very low frequency of reported wind speeds at 50 m from the NYSM LiDARs, this analysis is performed using wind speeds from 100 m and 250 m, which is sufficient to conform to the IEC standard recommendation that the shear be computed over a height differential of at least one-third of the rotor plane.

To capture LLJ that are of possible relevance to wind energy applications, LLJ are identified here as any wind speed profile that exhibits a vertically confined wind speed maximum in the lowest 500 m of the atmosphere with wind speeds above and below that level that are at least 2 ms^{-1} slower than in the maximum (Aird et al., 2021;Aird et al., 2022). This is to ensure the results are comparable to those reported previously for offshore regions of the U.S. east coast that used an analysis vertical window of 20 to 530 m (Aird et al., 2022).

3.4 Climatological context

Hourly zonal (*u*) and meridional (*v*) wind components at 10 and 100 m height are obtained for all ERA5 grid-cells in that contain NYSM and NYSERDA sites, and are converted to wind speed at 150 m height ($U150_{ERA5}$) using α derived from wind speeds at 10 and 100 m computed using equation (7). The mean shear exponent computed from wind speeds at 10 and 100 m height is 0.21, with variability over monthly and interannual timescales of less than 3 ~~percent~~%,~~1/7 which equates to~~ yielding a multiplier on the 100-m wind speed of 1.09 which is applied to obtain $U150_{ERA5}$~~6~~. Hourly $U150_{ERA5}$ estimates are used to calculate hourly wind production ($P150_{ERA5}$) using the IEA 15 MW reference wind turbine. The long-term records of $U150_{ERA5}$ and $P150_{ERA5}$ are used to assess the uncertainty in annual mean wind speeds and AEP resulting from the limited duration data records at the NYSM and NYSERDA LiDARs using a bootstrapping approach (Wilks, 2011). Hourly values from the 40-year $U150_{ERA5}$ and $P150_{ERA5}$ record are randomly resampled 1000 times with replacement using the number of hours from each month that the LiDAR data are available (Figure 3). For each of these 1000 bootstrapped samples the annual mean wind speed and AEP is calculated to provide an estimate of uncertainty that arises due to the short time series from the LiDARs. Additionally, Spearman correlation coefficients between the time series of $P150_{ERA5}$ at all NYSM and NYSERDA grid-cells are calculated for the full 44-year record and used to contextualize the spatial correlation derived using the LiDAR measurements.

3.5 LCoE

As indicated above there are many possible advantages in deploying wind turbines offshore as a component of the electricity generation system. One potential disadvantage is that offshore wind energy generation costs are expected to be higher than those from onshore wind, although still less than those from nuclear (Barthelmie et al., 2023). The simple Levelized Cost of Energy (LCoE) model applied here is similar to that developed in Barthelmie et al. (2023) ~~(Barthelmie et al., 2023)~~:

$$LCoE = \frac{CAPEX \cdot CRF + OPEX}{AEP} \tag{8}$$

where: *CAPEX* is the capital costs, *CRF* is the cost recovery factor, and *OPEX* is the annual operations and maintenance. Fixed costs are used here (Table 1), and *AEP* is the Annual Electricity Production from analyses described herein. Project lifetimes are assumed to be 30 years and no adjustment is made for turbine availability or other losses such as wakes or electrical losses. For the offshore locations, CAPEX is calculated from the values in Table 1 with no adjustments for distance to the coast, water depth, etc., and the water depth is appropriate for bottom-mounted wind turbines. Thus, the estimated LCoE from this simplified model are best case values.

Table 1. Key parameters for the LCoE model. Values taken from: (Stehly and Duffy, 2022).

	Onshore	Offshore
Capital expenditures (CAPEX) (million$/MW)	1.501	3.871
• Turbine (million$/MW)	1.03	1.3
• Fixed charge rate (%)	5.88	5.82
• Project costs (million$/MW)	0.120	0.67
• Foundation (million$/MW)	0.075	0.496
• Electric infrastructure including sub-stations (million$/MW)	0.132	0.693
• Finance ($/MW) (plus other costs for offshore includes e.g., decommissioning)	0.113	0.704
Operational expenditures (OPEX) ($/MW/yr)	0.04	0.111

4 Results

4.1 Wind resource, ~~and~~ potential power production, and LCoE

Wind speed time series from all the LiDARs (Table 2) indicate similar seasonality, consistent with their relative proximity. Highest monthly mean wind speeds at ~150 m occur during the cold season (November to March) and lowest values are observed during summer (July and August) (Figure 3). This is consistent with the climatology of the U.S. northeast with the cold season months exhibiting a high frequency of mid-latitude cyclone passages and with data from operating wind farms that exhibit highest CF during late winter and early spring (Pryor et al., 2023). The data also indicate considerably higher wind speeds at 150 m based on data from the LiDARs deployed offshore (Figure 3). The mean wind speeds at this height from the two NYSERDA buoy-mounted LiDARs are 10.1 ms^{-1}, while the mean wind speed from the Owego NYSM site (located < 400 km away) is 7.72 ms^{-1} (Table 2). In August, the mean monthly wind speed at the Hudson North buoy is 7.76 ms^{-1} and at Owego is 6.08 ms^{-1}; in December, the mean monthly wind speed at these two sites is 11.24 ms^{-1} and 9.16 ms^{-1}, respectively. Data from the LiDAR buoys also show a consistently higher frequency of U = 15-25 ms^{-1} when the IEA 15 MW reference wind turbine would operate at rated capacity (Figure 2). Figure 3 further indicates the presence of ~~a~~ seasonality in data availability. The excess representation of August in the Hudson North E05 data will tend to lead to a negative bias in the overall wind resource and estimated power production because wind speeds in that month are typically lower than other months (Figure 3). The mean monthly wind speed from August-November in data from the Hudson South E06 LiDAR is 9.75 ms^{-1}, which is below the overall mean, so the relatively low data availability in these months at E06 may also lead to a small negative bias in the derived mean energy density and power production (Figure 3). The seasonality in data availability is particularly consistent and amplified at the NYSM sites. As shown in Figure 3, at WANT (the site with the highest seasonal bias in data availability) over 12% of the total observations were recorded in July while in a data set free of availability bias this value would be 8.5%~~ranging from over 12% in summer to less than 6% in winter~~. Bootstrapping of ERA5 data indicates the mean annual wind speed computed from the LiDAR time series at the NYSM sites is likely underestimated by ~ 1.5-4.5% while AEP is underestimated by ~3-10% due to the high data availability in summer. Analyses of wind speed data from the NYSM LiDARs at all measurement heights from 100 to 500 m indicates that, averaged across all stations, the data availability as a function of height varies only by ±~~+/-~~2.5%.

Enquiries with the NYSM network operator did not resolve any common root cause for the low data availability from these LiDARs. Documentation associated with the data set notes the causes as; 'calibration errors; power failures; and/or communication failures.' And further notes 'Only manufacturer-developed QA/QC procedures are applied to the data and there might still be some undetected errors.' (readme accessible from http://www.nysmesonet.org/networks/profiler#stid=prof_alba). It is important to note that the differences in energy density computed from the on-shore and off-shore LiDAR data sets are robust to these sampling issues.

Table 2. Weibull distribution parameters from the 150 m wind speed time series (and 95% confidence intervals, CI) and energy density derived from those parameters. AEP computed using the IEA 15 MW wind turbine power curve, along with the frequency of zero power and power production at rated. The data shown in italics are computed using the most complete continuous 12-month period. The column headed e-folding time shows the time for the Spearman correlation coefficient to fall below e^{-1}. The ninth and tenth columns show the frequency of extreme shear for all periods when *U* at 150 m > 3 ms^{-1}. The following column shows estimated Levelized Cost of Energy (LCoE) values derived using the assumptions described in section 3.5 based on AEP estimates shown in the fifth column and derived using the LiDAR observations.

Site	Weibull Scale Parameter (A) (m/s) [CI]	Weibull Shape Parameter (k) [CI]	Energy Density (E) (W/m^2)	AEP (GWh/yr)	Frequency of no power production: *U* < 3 / U > 25 ms^{-1} (%)	Frequency of maximum (rated) power production (%)	e-folding time (hr)	Frequency of $\alpha < 0$	Freq of $\alpha > 0.3$	LCoE ($/MWh)
BRON	6.915 [6.896, 6.935]	2.013 [2.005, 2.021]	267	35.6	15.3/0.06	5.16	8.0	15.0	23.4	49.0
	7.146	*2.031*	*293*	*38.7*	*14.8/0.07*	*5.67*	*8.0*			
EHAM	10.16 [10.13, 10.18]	2.153 [2.144, 2.161]	794	71.7	6.38/0.31	21.2	9.3	15.4	17.0	26.0
	10.32	*2.202*	*816*	*73.0*	*5.63/0.40*	*23.1*	*9.3*			
OWEG	8.703 [8.678, 8.727]	2.172 [2.163, 2.181]	496	58.3	9.02/0.18	11.4	9.7	10.9	13.9	33.9
	8.514	*2.168*	*465*	*56.0*	*8.96/0.19*	*12.5*	*9.0*			
QUEE	7.607 [7.587, 7.627]	2.000 [1.993, 2.008]	358	43.3	12.2/0.14	8.66	8.8	19.0	17.3	45.3
	7.484	*2.009*	*340*	*41.9*	*13.0/0.12*	*7.75*	*7.8*			
STAT	7.602 [7.580, 7.625]	2.014 [2.006, 2.022]	355	43.6	12.4/0.14	6.49	7.2	15.9	20.2	43.7
	7.550	*2.029*	*345*	*43.4*	*13.0/0.12*	*6.17*	*7.3*			
STON	9.423 [9.396, 9.450]	2.039 [2.030, 2.048]	668	64.1	9.29/0.11	15.6	9.7	16.7	15.2	29.4
	9.447	*2.037*	*674*	*64.4*	*9.29/0.13*	*17.5*	*9.8*			

WANT	9.282 [9.254, 9.309]	1.970 [1.962, 1.977]	662	60.0	7.64/0.47	13.8	8.3	25.3	10.4	31.6
	9.185	*2.011*	*627*	*60.1*	*8.01/0.45*	*17.1*	*7.8*			
Hudson North E05	11.40 [11.36, 11.43]	2.127 [2.117, 2.137]	1134	79.7	5.30/0.48	30.6	11.3			61.9
	11.42	*2.147*	*1130*	*80.5*	*5.48/0.53*	*36.3*	*11.7*			
Hudson South E06	11.38 [11.34, 11.42]	2.123 [2.111, 2.134]	1131	80.0	5.94/0.46	27.2	10.0			64.4
	11.04	*2.073*	*1056*	*77.4*	*6.84/0.31*	*21.4*	*10.7*			

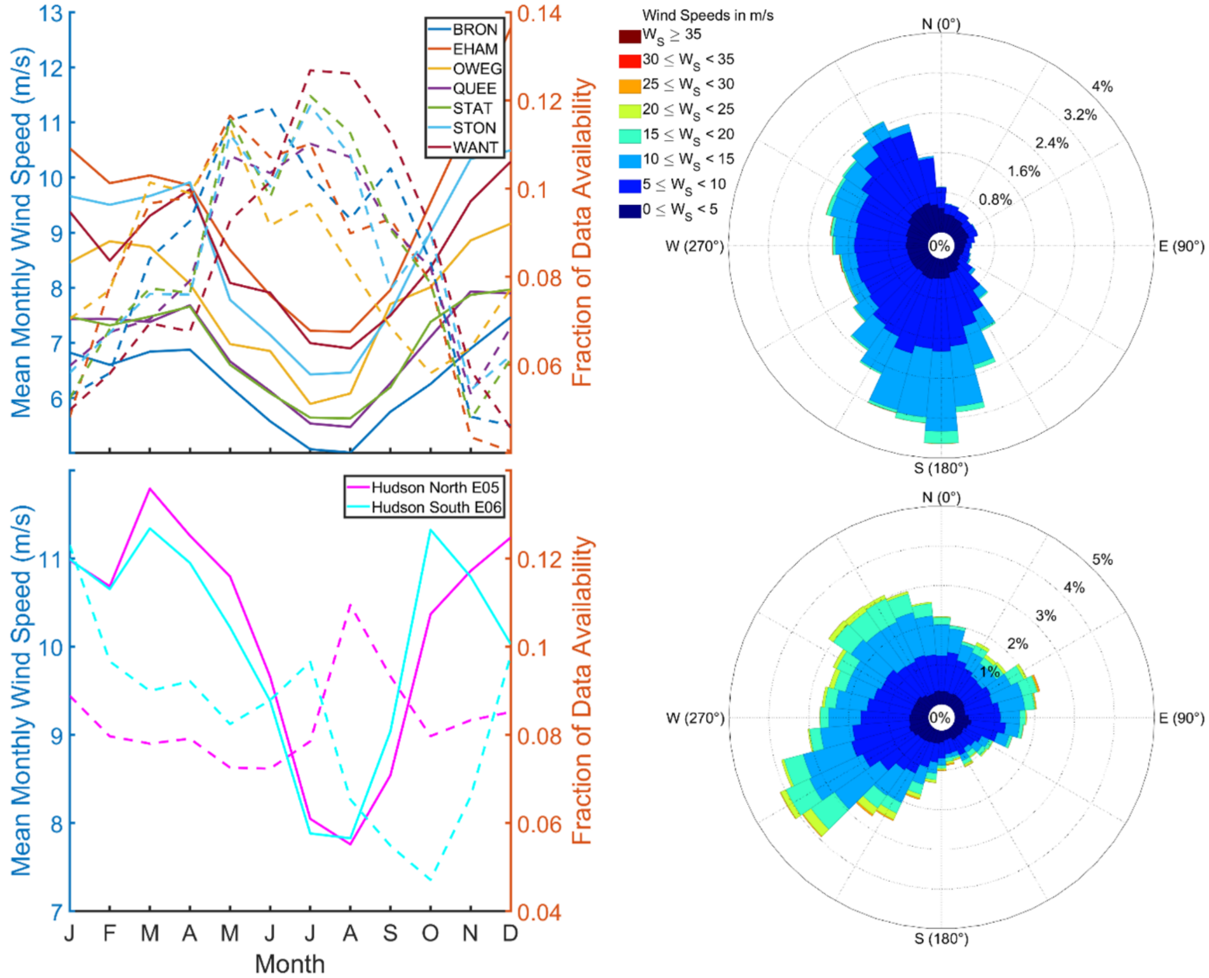

Figure 3. Monthly mean wind speed at ~150 m (ms^{-1}, solid lines) and fraction of data availability (dashed lines) for the seven NYSM sites with highest data availability (top left) and both NYSERDA buoy sites (bottom left), as well as wind roses for the OWEG (top right) and Hudson North E05 (bottom right) sites. A value of 0.08 for the fraction of data availability for a given month indicates 8% of the total sample is comprised of values recorded in that month.

The Weibull distribution fits to 150 m wind speeds from the buoy-mounted LiDARs have very similar shape and scale parameters (Figure 4 and Table 2). Consistent with expectations, the Weibull scale parameters from the NYSERDA buoys are also substantially higher than those from the seven NYSM sites and exceed values from the NYSM by 2 ms^{-1} for all sites except EHAM which is on Long Island and within 1 km of the coastline (Figure 1). The Weibull distribution parameters translate to higher energy densities at the locations of the buoys (Table 2). This is also true for calculations based on the 'best year' of data (Table 2). When wind speeds from the 'best year' are used to compute the Weibull fits and AEP, differences of 0.1-3% in the Weibull scale parameters and 1-8% in AEP are found relative to estimates from the longest available records (Table 2). Even compared to the NYSM location with the highest Weibull scale parameter and highest mean wind speeds (EHAM), both buoys have over 40% higher energy density. Application of the power curve from the IEA 15 MW reference turbine to the wind speed time series yields AEP values for the buoy-mounted LiDARs that are a factor of almost three higher than some of the NYSM sites (e.g., QUEE and STAT) and nearly twice as much as many NYSM stations except EHAM (Table 2). Thus, consistent with expectations, the wind speed time series from the LiDARs operated on the NYSERDA buoys indicate a substantially better wind resource and higher projected electrical power output (AEP) than is estimated based on data from the NYSM LiDARs.

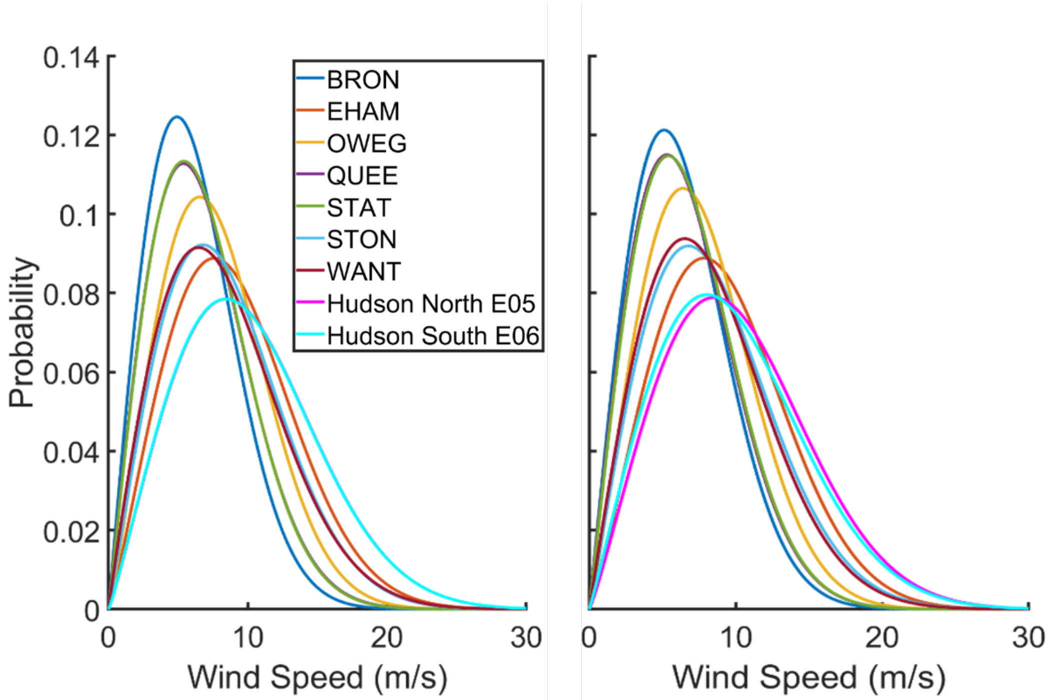

Figure 4. Probability distributions from the Weibull fits to 10-minute wind speeds at 150 m height from the NYSERDA LiDAR buoys and the NYSM stations for all available data (left) and year with common highest data availability ('best year' of September 2018-2019) (right). Note: probability distributions from Hudson North E05 and Hudson South E06 virtually overlay each other in the left panel.

Despite higher projected AEP for the offshore locations, the additional costs involved in installing and operating offshore wind farms results in higher LCoE estimates for the offshore sites (Table 2). LCoE estimates derived using AEP at the NYSM sites and assumptions stated in section 3.5 (Table 1) are 26 to 49 \$/MWh while estimates for the NYSERDA buoy locations are 62-64 \$/MWh.

4.2 Power quality

Three aspects of power quality are evaluated using the wind speed at ~150 m (U) and power production time series. The first is the probability of wind speeds at which no power is produced; $U < 3$ ms^{-1} or $U > 25$ ms^{-1}. The probabilities of wind speeds below the cut-in speed of the IEA 15 MW wind turbine ($U < 3$ ms^{-1}) are substantially higher for the NYSM sites than the offshore locations (Table 2 and Figure 4). Indeed, for three of the seven NYSM sites the probability of wind speeds below cut-in is well over twice that for the offshore sites, and even the locations of Long Island that are very close to the coast (EHAM and WANT) exhibit considerably higher frequency of $U < 3$ ms^{-1} than is derived using data from NYSERDA LiDARs (7.6 and 6.4% versus 5.3 and 5.9%, see Table 2). The frequency of U above cut-out ($U > 25$ ms^{-1}) is higher based on data from the LiDARs on the buoys, but the overall frequency is low at all locations (< 0.5%). Thus, wind turbines deployed offshore at the NYSERDA buoy locations will produce some power on a considerably larger fraction of the time than any of the onshore locations. This inference is true whether the entire time series or the "best year" of data are considered.

The second component of power quality is the intermittency in terms of the probability and magnitude of ramp events – that is rapid changes in wind speed and/or power production. Wind speed time series at 150 m height from the NYSM and NYSERDA LiDARs indicate clear similarities in terms of ramp event magnitude and frequency to those derived using data from the FINO1 platform in the North Sea, Cabauw onshore in western portion of the Netherlands, Høvsøre in coastal Jutland, Denmark, and NWTC in the foothills of the Colorado Rocky Mountains (DeMarco and Basu, 2018) (Figure 5). Data from the NYSERDA buoys indicate a low probability of wind speed ramps of all magnitudes relative to the NYSM LiDARs (Figure 5), and all LiDAR time series indicate a substantially higher probability of a ramp-up (increase) than a ramp-down (decrease) of a given magnitude in wind speeds. Wind speed ramps in hourly ERA5 data exhibit a narrower distribution owing to spatial and temporal averaging, illustrating the need for in-situ data for capturing high resolution wind variability (Figure 5). Consistent with the lower probability of large-magnitude rapid changes in wind speed offshore, d~~D~~ata from the NYSERDA buoys (Hudson North E05 and Hudson South E06) indicate probabilities of a wind power ramp with > ±20% change in power are considerably lower than those from any of the onshore locations (Figure 5). Thus, the chance of experiencing an increase or decrease in electrical power production of 20% from one 10-minute period to the next is substantially lower for wind turbines deployed offshore. ~~indicating~~ This indicates that wind turbines deployed offshore are likely to exhibit less intermittency in terms of electrical power production which is critical to efficient grid integration (Ayodele et al., 2012).

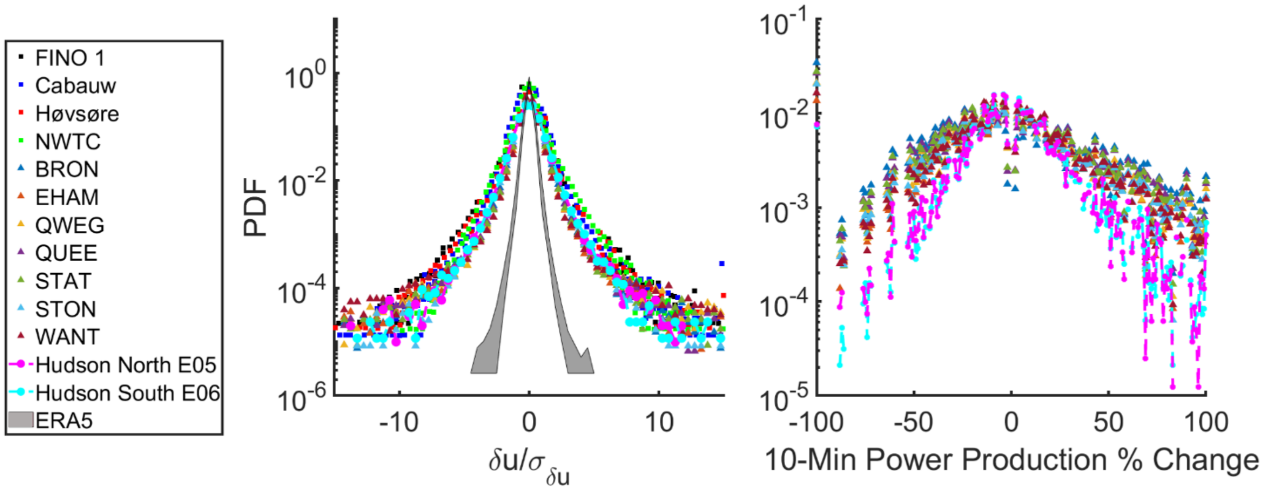

Figure 5. Left: probabilities of wind speed ramp events computed from the 10-minute data from the NYSERDA LiDAR buoys and the NYSM sites computed using Equation (3), and reported for four locations at or near operating wind turbines: FINO 1 is (offshore) in the North Sea, Cabauw is in the western portion of the Netherlands, Høvsøre is in Jutland, Denmark, and NWTC is in the foothills of the Colorado Rocky Mountains (data digitized from: (DeMarco and Basu, 2018)). Wind ramps computed from the hourly ERA5 output are shown by the gray polygon. Right: probabilities of wind power production ramp events at the locations of the NYSERDA buoys and the NYSM sites computed by applying the power curve for the IEA 15 MW reference wind turbine to the LiDAR wind speeds. The probabilities of no-change (i.e., power ± 0%) are not shown to aid visibility.

The third aspect of power quality is predictability. The autocorrelation in power production at different time lags for the NYSM LiDARs exhibit clear diurnal oscillations and shorter e-folding time scales. Power production estimates using wind speeds from the Hudson North E05 buoy show the largest e-folding time of ~68, 10--minute periods (11.3 hours), and ~70, 10--minute periods (11.7 hours) in the 'best year' of data. Comparable estimates for data from the Hudson South E06 buoy are ~ 60 and 64, 10--minute periods (10.0 and 10.7 hours) (Table 2 and Figure 6). These relatively large e-folding times for the buoy locations indicate a longer atmospheric 'memory' at these sites, indicating the potential for more accurate short-term power prediction forecasts because each time step is strongly dependent on the value in previous time step(s).

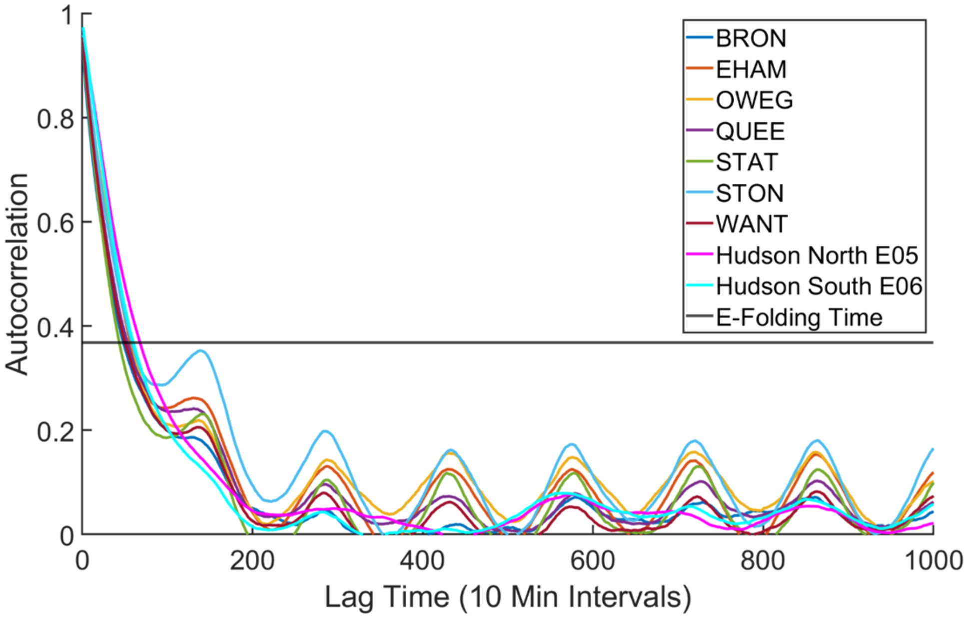

Figure 6. Temporal autocorrelation (computed using Spearman correlation coefficients) of the wind power production at different lag times based on data from the NYSERDA buoys and the NYSM stations. The horizontal line denotes a correlation of e^{-1} which is used here as a first order estimate of the e-folding time.

4.3 Spatial correlation

While power production from wind farms is inherently intermittent at the local scale, aggregation over large spatial scales reduces power fluctuations (Potisomporn and Vogel, 2022;Pryor et al., 2014;Simão et al., 2017;Pryor et al., 2020b;St. Martin et al., 2015). However, the optimal spatial scale of integration is likely to be a strong function of the prevailing meteorology. Thus, an analysis of power production computed based on LiDAR data at each of the NYSM profiler stations and NYSERDA buoys is undertaken to quantify the spatial decorrelation scale. Consistent with the a priori expectation based on past research, the correlation of time-series of estimated power production at the different locations decays exponentially with increasing separation distance (Figure 7). The highest correlation coefficient is between power production time series from the two NYSERDA buoys (0.834, see SM Table 1 and Figure 7). NYSM sites EHAM and STON have an almost identical separation distance as the buoys (Figure 1), but these time series of estimated power production have a slightly lower correlation coefficient (0.764) due to variability caused by the presence of land use land cover and terrain features onshore. For the sample sizes of data from the LiDARs and a lag-1 autocorrelation of > 0.9, application of equations (4) and (5) imply the power production time series would be considered fully de-correlated at Spearman correlation coefficients < 0.2. As shown in Figure 7 this level is not reached for the sites at which the LiDAR are deployed. Nevertheless, exponential fits to correlation coefficients as a function of separation distance imply that on average the correlation coefficients drop below about 0.4 for separation distances of ~ 350 km. This suggests that careful siting of wind farms on- and off- shore could be used to decrease coherent variations in electrical power production within the NY ISO. Output from ERA5 when converted to electrical power production exhibits higher correlation coefficients at similar separation distances to the LiDARs consistent with the higher spatial smoothing inherent in reanalysis products (Figure 7).

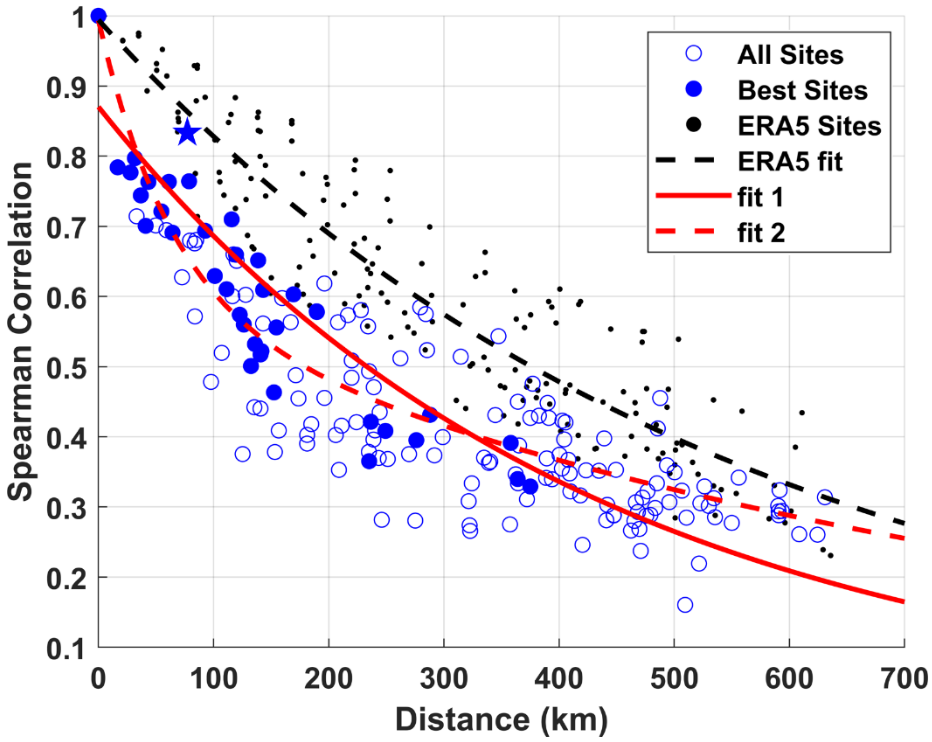

Figure 7. Spearman spatial correlation coefficient (*r*) of power production for the LiDAR (blue) and ERA5 (black) output sampled at the NYSERDA and NYSM locations against the separation distance between all 19 sites (17 onshore, 2 offshore). Solid blue points indicate location pairs with high data availability, open points represent the relationships including the remaining NYSM sites. The star represents the correlation between the two NYSERDA buoys. Best fit lines (y = Spearman correlation coefficient, x = spherical distance between locations) are shown for the LiDAR: y = 0.8703exp(-0.002377x) (solid red) and y = 0.4021exp(-0.01595x) + 0.5914exp(-0.0012x) (dashed red). The fit to the ERA5 estimates has the form y = 0.9942exp(-0.00183x) (dashed black).

4.4 Shear conditions and LLJ at the NYSM onshore sites

LiDAR data from all 17 NYSM sites indicate a very high frequency of extreme wind shear (Table 2). This is likely due in part to the heights being considered lying outside of the surface layer when the wind power law is most likely to be an appropriate approximation. Nevertheless, all NYSM LiDARs have a very high frequency of shear exponents computed using wind speeds at 100 and 250 m for wind speeds at 150 m of 3 to 25 ms^{-1} that lie beyond the 0 to 0.3 expected range. At all the NYSM sites, 5% of shear exponent values during wind turbine operation lie above 0.39 and a further 5% of values fall below -0.09. The high frequency of extreme positive shear at many of the sites is likely to be due to the high surface roughness lengths since many of the NYSM sites are in the southeast of the state in highly urbanized locations. The frequency of negative shear is highest at WANT, on Long Island, likely in part because of the local land use land cover variability. The occurrence of negative shear 10.9-25.0% of the time from the NYSM sites is broadly comparable to the frequency of occurrence of negative shear between heights of 42-292 m (12%) found in WRF simulations over the U.S. state of Iowa (Barthelmie et al., 2020). A high positive shear exponents (α > 0.2) was also found in analyses of WRF output in Iowa (>38%) again consistent with the estimated probability of occurrence derived using the NYSM LiDAR data (100 to 250 m) (Table 2). The implication is that large wind turbines deployed in these locations may experience a relatively high frequency of large unbalanced rotor loads and reduced component lifetimes unless such loads can be appropriately compensated (Hur et al., 2017).

Consistent with the lower wind speeds during the summer (Figure 3), weaker synoptic forcing during this season, and previous analyses of LLJ offshore (Aird et al., 2022), all NYSM sites exhibit the highest frequency of LLJ occurrence in the summer months (Figure 8). The highest frequency of occurrence (14% of all 10-minute periods) of LLJ occurs during June at EHAM on the coast of Long Island (Figure 8). Analyses of the WRF simulations for this location found a LLJ frequency during June of 11% and a very similar seasonal cycle of occurrence (Aird et al., 2022). The site-to-site variability in LLJ probability at the different NYSM locations is due to local site conditions (e.g., proximity to the coastline, topographic variability and land use land cover variability) that are linked to the dynamical causes of LLJ (Balsley et al., 2003;Kallistratova et al., 2009;Blackadar, 1957;Holton, 1967). LLJ core heights are also lower during the summer months, with LiDAR observations from WANT indicating a mean LLJ core height of < 280 m during June (Figure 8). However, for most of the NYSM locations the mean LLJ core heights are above 300 m and thus above the swept area even of the IEA 15 MW reference wind turbine. There is a higher probability of LLJ intersecting with the rotor plane during summer. However, LLJ diagnosed from the onshore LiDARs are typically at greater elevations than are indicated offshore by the WRF simulations, where LLJ cores were frequently < 200 m above the sea surface (Aird et al., 2022). It is important to acknowledge that comparisons of LLJ climates derived from LiDAR measurements and WRF modelling should be done cautiously and that LLJ detection from the LiDAR wind speed profiles is critically dependent on unbiased data availability. Nevertheless, this analysis suggests LLJ within the rotor plane, as a source of ~~large unbalanced~~large, unbalanced rotor loads and reduced blade lifetimes, are less frequent at these onshore locations.

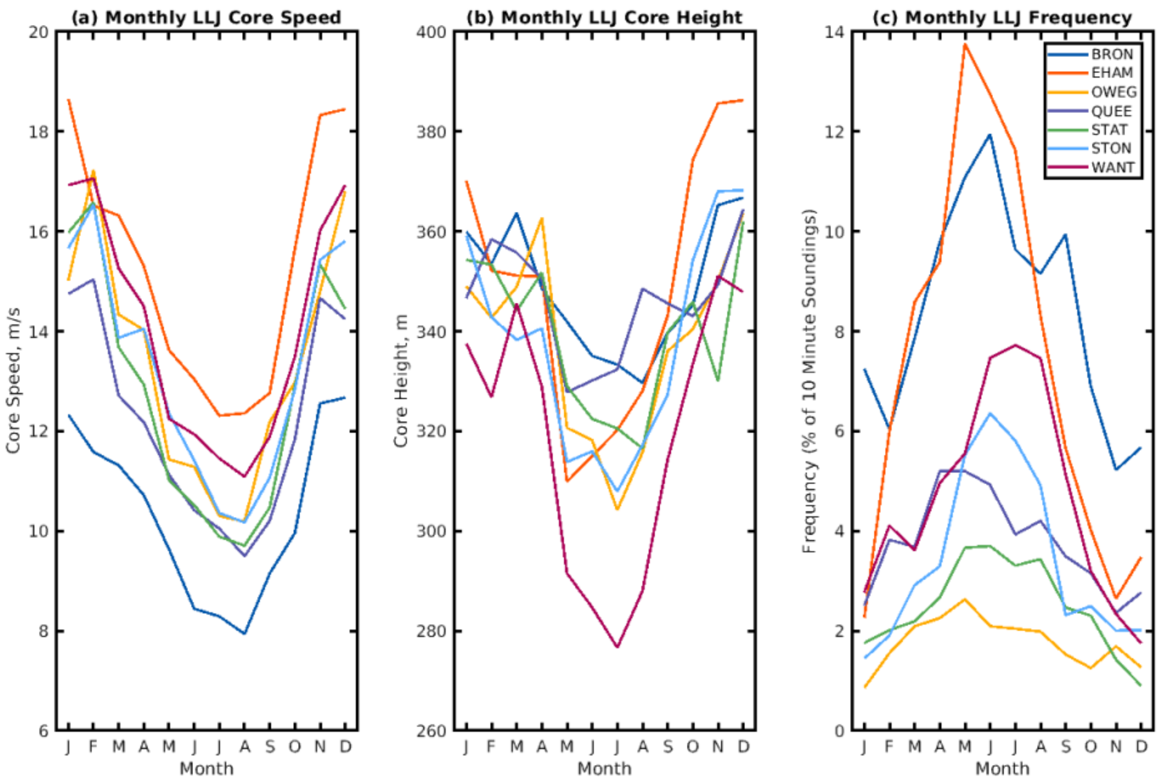

Figure 8. Monthly mean low-level jet (a) core wind speed (ms^{-1}), (b) core height (m), and (c) the mean frequency of occurrence (probability of occurrence in any given 10-minute LiDAR profile) across the seven NYSM sites. A LLJ frequency of 5% calculated from the LiDAR deployed at QUEE for the calendar month of May indicates that LLJ were indicated in 5% of all 10-minute periods during this month. Data in panels (a) and (b) indicate that at that site in the month of May the associated LLJ mean core wind speed is 11 ms^{-1} and the mean core height above ground is 3340 m.

4.5 Demand matching

Electricity demand in New York state tends to peak in the afternoon (~ 1700 eastern standard time, EST) and in summer (highest values in July), though a secondary maximum occurs in January (Figure 9). Wind power production calculated from the NYSM/NYSERDA LiDARs and ERA5 grid-cell data ($P150_{ERA5}$) show highest values at night (0100 to 0500 EST) and during winter to spring (December-April), with the lowest production during the day (1300 to 1600 EST) and during the summer (Figure 9). Wind power production estimated based on LiDAR data from the NYSERDA buoy locations exhibits markedly lower diurnal and seasonal variability than is estimated at the NYSM sites, varying by ± 10% around the mean versus ± 25% at NYSM. This results in a reduction in mean absolute error (MAE) between time series of normalized WPP from the offshore LiDAR and electricity demand on both diurnal and seasonal timescales. The MAE computed from the mean hourly offshore WPP and demand is 0.19 when computed over the 24 hours of the day (Figure 9a) and 0.13 when computed from the time series of monthly mean values (Figure 9b). Both are smaller than MAE computed from WPP from the onshore LiDARs and demand on these time scales which are 0.25 and 0.20, respectively. This implies there will be better matching to electricity demand for power production from wind turbines deployed offshore~~-~~.

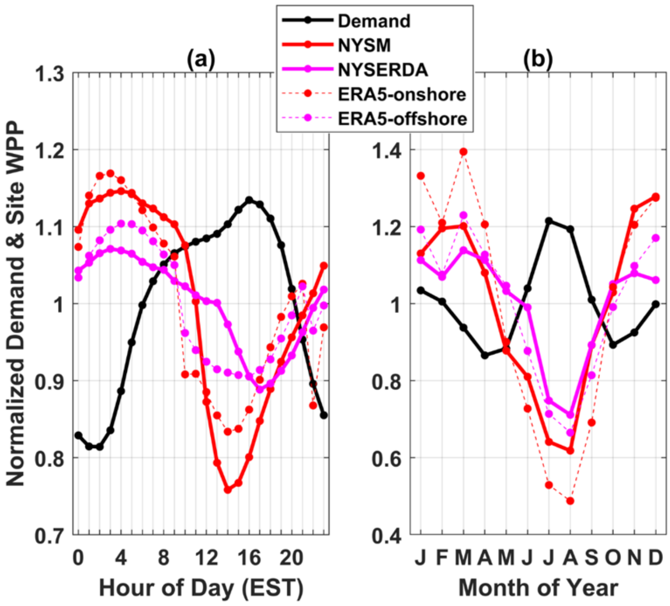

Figure 9. Normalized (a) diurnal and (b) monthly cycles of electricity demand for New York State (black) and wind power production (WPP) at NYSM (red) and NYSERDA (magenta) sites. ERA5-derived WPP is shown for the grid-cells which contain the NYSM and NYSERDA LiDARs (thin, dashed lines) for the climatological period, 1979-2022. The data are normalized to a mean value of 1 and so that values of 0.9 or 1.1 in a given hour or month indicates WPP or demand that is 10% below or above the mean, respectively.

5 Concluding remarks

~~Very few detailed cQuantitative c~~Comparative analyses of wind resources and projected power production quantity and quality at onshore and offshore locations ~~are available in the literature due largely to the limited~~have been hampered by the lack of high-quality ~~availability of~~ hub-height wind speed observations. Here we use uniquely detailed LiDAR measurements from an onshore profiler network and offshore campaign to compare projections of potential power generation quantity and quality from offshore and onshore locations in New York State (Figure 1). ~~The~~ Returning to the ~~study~~ objectives articulated in section 1, the study results indicate there are significant benefits to offshore deployments of wind turbines:

- Wind resources at locations in the New York Bight (coastal offshore areas southeast of New York state, Figure 1) greatly exceed those of all onshore locations within New York state. The mean wind speeds at ~150 m ($\overline{U}$) offshore are above 10 ms^{-1}, while $\overline{U}$ is below 8 ms^{-1} at all onshore sites. Weibull distribution fits to the 10-minute wind speed time series indicate scale parameters that are higher by 2 ms^{-1} than all onshore locations (Figure 4) except EHAM which is on Long Island and is within 1 km of the coastline (Figure 1). Accordingly, energy densities are 40% higher offshore and power production estimated offshore using the power curve of the IEA 15 MW wind turbine (Figure 2) yield over twice the AEP estimated for all onshore sites except EHAM (Table 2). Power generation estimated from wind speed time series offshore also exhibits lower variability on diurnal and seasonal time scales (Figure 6) and improved matching to current electricity demand in New York ~~State~~ state (Figure 9). This implies that not only is the offshore resource considerably larger offshore, but the ability to meet electricity demand is better for wind turbines deployed offshore.
- Analyses presented herein also suggest that power generation intermittency is lower for the offshore sites. The probability of wind speeds below cut-in or above cut-out for the IEA reference wind turbine is lower offshore, as is the probability of large magnitude wind speed and power ramps (Figure 5). For example, the probabilities of wind power ramps with > ±20% change in power over a 10-minute period are less than half as probable offshore as onshore.

The higher temporal autocorrelation of wind power production offshore (Figure 6 and Table 2) may also aid the accuracy of short-term wind power forecasting for wind turbines deployed offshore, yielding economic benefits to wind farm owner/operators and enabling grid integration.

Conversely, t~~T~~he frequency of anomalous wind speed shear and LLJ close to, or within, the rotor plane computed from the NYSM LiDAR wind speed profiles are slightly higher than those previously reported for the offshore areas from numerical simulations (Aird et al., 2022) but LLJ also exhibit higher elevations of the jet cores (Figure 8) and thus may be of less concern to wind turbine loading.

An analysis of the distance dependence of the co-variability of power production derived from measured 10-minute mean wind speed time series at the onshore and offshore sites indicates that the non-parametric Spearman correlation coefficient drops below 0.4 at distances of about 350 km (Figure 7). This ~~indicates~~implies that in order to ensure consistency of electrical power production from wind farms in New York state, major developments should be separated by more than 350 km. This information could be used to guide judicious selection of wind farm locations ~~can be used~~ to minimize the probability of concurrent low generation from onshore and offshore sites.

~~In~~ Thus, in accord with a priori expectations, analyses presented herein indicate there are advantages to the emerging trend towards offshore wind energy deployments in terms of the wind resource and the expected power quality and predictability (reduced ramp events, higher probability of rated power, etc.). Despite higher project AEP for the offshore locations, the additional costs involved in installing and operating offshore wind farms results in higher LCoE estimates for the offshore sites (Table 2). LCoE estimates derived using AEP at the NYSM sites ~~and assumptions stated in section 3.5 (Table 1)~~ are 26 to 49 \$/MWh while estimates for the NYSERDA buoy locations are 62-64 \$/MWh. Nevertheless, projected LCoE from wind energy for all of the sites investigated here in NY are competitive with all other electricity generation sources, with the possible exception of utility-scale PV, and much less expensive than traditional sources such as coal and nuclear that, according to a recent analysis, have an unsubsidized LCoE of 65-152 \$/MWh and 131-204 \$/MWh, respectively (Lazard, 2023).

6 Code availability

Analyses presented here were performed using normal functions within MATLAB™. No specialized codes were developed or employed.

7 Data availability

The LiDAR data from the NYSERDA buoy campaign are available from: NYSERDA (2022). *E05 Hudson North 10 Minute*. Det Norske Veritas. Retrieved February 13, 2022, from https://oswbuoysny.resourcepanorama.dnvgl.com/download/f67d14ad-07ab-4652-16d2- 08d71f257da1 and NYSERDA (2022). *E06 Hudson South 10 Minute*. Det Norske Veritas. Retrieved February 13, 2022, from https://oswbuoysny.resourcepanorama.dnvgl.com/download/f67d14ad-07ab-4652-16d2- 08d71f257da1 . Reports documenting LiDAR performance verification are also available for download from: https://oswbuoysny.resourcepanorama.dnv.com/download/f67d14ad-07ab-4652-16d2-08d71f257da1. Specifications for the 15 MW reference wind turbine are available from *GitHub - IEA Wind Task 37/IEA-15-240-RWT*. https://github.com/IEAWindTask37/IEA-15-240-RWT. Data from the New York State Mesonet can be requested from: http://www.nysmesonet.org/. A readme documenting data processing for this network is available from: http://www.nysmesonet.org/networks/profiler#stid=prof_alba. ERA5 reanalysis products can be downloaded from https://cds.climate.copernicus.eu/#!/home.

8 Author contribution

SCP conceptualized the study, managed the project and acquired the data sets used in the study. SCP and RJB acquired the funding and the computing resources used. RF, SCP, JCC, RJB and JAA performed data analyses. RF and JCC led the visualization. RF and SCP wrote the initial draft. All authors contributed to refinement of the final manuscript.

9 Competing interests

RJB is a member of the editorial board of Wind Energy Science. The peer-review process was guided by an independent editor, and the authors have also no other competing interests to declare.

10 Acknowledgements

The authors are grateful for funding from the U.S. Department of Energy Office of Science (DE-SC0016605), the U.S. Department of Energy Office of Energy Efficiency and Renewable Energy, and the New York State Energy Research and Development Authority via the National Offshore Wind Research and Development consortium (147505 and 147506). This research was further enabled by computational resources supported by the U.S. National Science Foundation via the Extreme Science and Engineering Discovery Environment (XSEDE) (award TG-ATM170024). This research was made possible in part by the New York State (NYS) Mesonet. Original funding for the NYS Mesonet was provided by Federal Emergency Management Agency grant FEMA-4085-DR-NY, with the continued support of the NYS Division of Homeland Security & Emergency Services; the State of New York; the Research Foundation for the State University of New York (SUNY); the University at Albany; the Atmospheric Sciences Research Center (ASRC) at the University at Albany; and the Department of Atmospheric and Environmental Sciences (DAES) at the University at Albany.

11 References

Aird, J. A., Barthelmie, R. J., Shepherd, T. J., and Pryor, S. C.: WRF-Simulated Low-Level Jets over Iowa: Characterization and Sensitivity Studies, Wind Energy Science, 6, 1015-1030, 10.5194/wes-6-1015-2021, 2021.

Aird, J. A., Barthelmie, R. J., Shepherd, T. J., and Pryor, S. C.: Occurrence of Low-Level Jets over the Eastern US Coastal Zone at Heights Relevant to Wind Energy, Energies 15, 445, 10.3390/en15020445, 2022.

American Clean Power: Clean Power Quarterly 2023 Q1, Available for puchase from: https://cleanpower.org/resources/clean-power-quarterly-report-q1-2023/, 135, 2023.

Ayodele, T. R., Jimoh, A., Munda, J. L., and Tehile, A. J.: Challenges of grid integration of wind power on power system grid integrity: A review, International Journal of Renewable Energy Research, 2, 618-626, 2012.

Balsley, B. B., Frehlich, R. G., Jensen, M. L., Meillier, Y., and Muschinski, A.: Extreme gradients in the nocturnal boundary layer: Structure, evolution, and potential causes, Journal of the Atmospheric Sciences, 60, 2496-2508, 2003.

Bamigbola, O. M., Ali, M. M., and Oke, M. O.: Mathematical modeling of electric power flow and the minimization of power losses on transmission lines, Applied Mathematics and Computation, 241, 214-221, 2014.

Barthelmie, R. J., Grisogono, B., and Pryor, S. C.: Observations and simulations of diurnal cycles of near-surface wind speeds over land and sea, Journal of Geophysical Research, 101, 21,327-321,337, 10.1029/96JD01520, 1996.

Barthelmie, R. J., Murray, F., and Pryor, S. C.: The economic benefit of short-term forecasting for wind energy in the UK electricity market, Energy Policy 36, 1687–1696, 2008.

Barthelmie, R. J., Doubrawa, P., Wang, H., Giroux, G., and Pryor, S. C.: Effects of an escarpment on flow parameters of relevance to wind turbines, Wind Energy, 19, 2271-2286, 2016.

Barthelmie, R. J., Shepherd, T. J., Aird, J. A., and Pryor, S. C.: Power and wind shear implications of large wind turbine scenarios in the U.S. Central Plains, Energies, 13, 4269 doi: 4210.3390/en13164269, 2020.

Barthelmie, R. J., Larsen, G. C., and Pryor, S. C.: Modeling Annual Electricity Production and Levelized Cost of Energy from the US East Coast Offshore Wind Energy Lease Areas, Energies, 16, 4550, 2023.

Bingöl, F., Mann, J., and Larsen, G. C.: Light detection and ranging measurements of wake dynamics part I: one-dimensional scanning, Wind Energy, 13, 51-61, 10.1002/we.352, 2010.

Bischoff, O., Wurth, I., Gottschall, J., Gribben, B., Hughes, J., Stein, D., and Verhoef, H.: Floating Lidar Systems, IEA Expert Group Report on Recommended Practices, IEA Wind TCP RP 18 from Task 32. Available for download from: https://iea-wind.org/portfolio-item/recommended-practice-18/, 89, 2017.

Bistline, J. E., and Blanford, G. J.: The role of the power sector in net-zero energy systems, Energy and Climate Change, 2, 100045, 2021.
Blackadar, A. K.: Boundary layer wind maxima and their significance for the growth of nocturnal inversions, Bulletin of the American Meteorological Society, 38, 283-290, 1957.
BOEM: Outer Continental Shelf Renewable Energy Leases Map Book, Available for download from: https://www.boem.gov/sites/default/files/documents/renewable-energy/Outer%20Continental%20Shelf%20Renewable%20Energy%20Leases%20January%202023b.pdf Accessed 14 March 2023. 33pp, 2023.
Brotzge, J. A., Wang, J., Thorncroft, C., Joseph, E., Bain, N., Bassill, N., Farruggio, N., Freedman, J., Hemker Jr, K., and Johnston, D.: A technical overview of the New York State Mesonet standard network, Journal of Atmospheric and Oceanic Technology, 37, 1827-1845, 2020.
Burleyson, C. D., Rahman, A., Rice, J. S., Smith, A. D., and Voisin, N.: Multiscale effects masked the impact of the COVID-19 pandemic on electricity demand in the United States, Applied Energy, 304, 117711, 2021.
Castillo, V. Z., De Boer, H.-S., Muñoz, R. M., Gernaat, D. E., Benders, R., and van Vuuren, D.: Future global electricity demand load curves, Energy, 258, 124741, 2022.
Coburn, J. J., and Pryor, S. C.: Projecting future energy production from operating wind farms in North America: Part 3: Variability, Journal of Applied Meteorology and Climatology In review, 2023.
DeMarco, A., and Basu, S.: On the tails of the wind ramp distributions, Wind Energy, 21, 892-905, 2018.
Diógenes, J. R. F., Claro, J., Rodrigues, J. C., and Loureiro, M. V.: Barriers to onshore wind energy implementation: A systematic review, Energy Research & Social Science, 60, 101337, 2020.
Enevoldsen, P., and Jacobson, M. Z.: Data investigation of installed and output power densities of onshore and offshore wind turbines worldwide, Energy for Sustainable Development, 60, 40-51, 10.1016/j.esd.2020.11.004, 2021.
Eryilmaz, D., Patria, M., and Heilbrun, C.: Assessment of the COVID-19 pandemic effect on regional electricity generation mix in NYISO, MISO, and PJM markets, The Electricity Journal, 33, 106829, 2020.
Esteban, M. D., Diez, J. J., López, J. S., and Negro, V.: Why offshore wind energy?, Renewable energy, 36, 444-450, 2011.
Gadde, S. N., Liu, L., and Stevens, R. J.: Effect of low-level jet on turbine aerodynamic blade loading using large-eddy simulations, Journal of Physics: Conference series, 2021, 012001, doi: 012010.011088/011742-016596/011934/012001/012001,
Gaertner, E., Rinker, J., Sethuraman, L., Zahle, Z., Anderson, B., Barter, G., Abbas, B., Meng, F., Bortolotti, F., Skrzypinski, W., Scott, G., Feil, R., Bredmose, H., Dykes, K., Shields, M., Allen, G., A., V., and 2020.: Definition of the IEA 15-Megawatt Offshore Reference Wind Turbine, National Renewable Energy Laboratory, Golden, CO. NREL/TP-5000-75698. Available for download from: https://www.nrel.gov/docs/fy20osti/75698.pdf, 2020.
Gramcianinov, C. B., Campos, R. M., de Camargo, R., Hodges, K. I., Guedes Soares, C., and da Silva Dias, P. L.: Analysis of Atlantic extratropical storm tracks characteristics in 41 years of ERA5 and CFSR/CFSv2 databases, Ocean Engineering, 216, 108111, 10.1016/j.oceaneng.2020.108111, 2020.
Gutierrez, W., Ruiz-Columbie, A., Tutkun, M., and Castillo, L.: The structural response of a wind turbine under operating conditions with a low-level jet, Renewable and Sustainable Energy Reviews, 108, 380-391, 2019.
Haghi, H. V., Bina, M. T., and Golkar, M. A.: Nonlinear modeling of temporal wind power variations, IEEE Transactions on Sustainable Energy, 4, 838-848, 2013.
Hallgren, C., Arnqvist, J., Ivanell, S., Körnich, H., Vakkari, V., and Sahlée, E.: Looking for an offshore low-level jet champion among recent reanalyses: a tight race over the Baltic Sea, Energies, 13, 3670, 2020.
Haslett, J., and Raftery, A. E.: Space-time modelling with long-memory dependence: Assessing Ireland's wind power resource, Journal of the Royal Statistical Society: Series C (Applied Statistics), 38, 1-21, 1989.
Hersbach, H., Bell, B., Berrisford, P., Hirahara, S., Horányi, A., Muñoz-Sabater, J., Nicolas, J., Peubey, C., Radu, R., Schepers, D., Simmons, A., Soci, C., Abdalla, S., Abellan, X., Balsamo, G., Bechtold, P., Biavati, G., Bidlot, J., Bonavita, M., De Chiara, G., Dahlgren, P., Dee, D., Diamantakis, M., Dragani, R., Flemming, J., Forbes, R., Fuentes, M., Geer, A., Haimberger, L., Healy, S., Hogan, R. J., Hólm, E., Janisková, M., Keeley, S., Laloyaux, P., Lopez, P., Lupu, C., Radnoti, G., de Rosnay, P., Rozum, I., Vamborg, F., Villaume, S., and Thépaut, J.-N.: The ERA5 global reanalysis, Quarterly Journal of the Royal Meteorological Society, 146, 1999-2049, 10.1002/qj.3803, 2020.
Holton, J. R.: The diurnal boundary layer wind oscillation above sloping terrain, Tellus, 19, 200-205, 1967.
Hur, S., Recalde-Camacho, L., and Leithead, W.: Detection and compensation of anomalous conditions in a wind turbine, Energy, 124, 74-86, 2017.
IEA: Wind Electricity, International Energy Agency, Paris, Available for download from: https://www.iea.org/reports/wind-electricity, 2022.
IEC: IEC 61400-1 Edition 4.0 2019-02 Wind turbines – Part 1: Design requirements, International Electrotechnical Commission, Geneva, Switzerland. ISBN 978-2-8322-6253-5, Geneva, Switzerland, 168 pp., 2019.
Irwin, J. S.: A theoretical variation of the wind profile power-law exponent as a function of surface roughness and stability, Atmospheric Environment, 13, 191-194, 1979.
Kallistratova, M., Kouznetsov, R. D., Kuznetsov, D. D., Kuznetsova, I. N., Nakhaev, M., and Chirokova, G.: Summertime low-level jet characteristics measured by sodars over rural and urban areas, Meteorologische Zeitschrift, 18, 289-295, 2009.
Kariniotakis, G., Pinson, P., Siebert, N., Giebel, G., and Barthelmie, R.: The state of the art in short term prediction of wind power-from an offshore perspective, SeaTech Week-Ocean Energy Conference ADEME-IFREMER, Brest, France, 2004, 13,
Kelberlau, F., and Mann, J.: Quantification of motion-induced measurement error on floating lidar systems, Atmospheric Measurement Techniques, 15, 5323-5341, 2022.

Kiviluoma, J., Holttinen, H., Weir, D., Scharff, R., Söder, L., Menemenlis, N., Cutululis, N. A., Danti Lopez, I., Lannoye, E., and Estanqueiro, A.: Variability in large-scale wind power generation, Wind Energy, 19, 1649-1665, 2016.
Kumer, V.-M., Reuder, J., Dorninger, M., Zauner, R., and Grubišić, V.: Turbulent kinetic energy estimates from profiling wind LiDAR measurements and their potential for wind energy applications, Renewable Energy, 99, 898-910, 2016.
Lazard: Lazard's Levelized Cost of Energy Analysis—Version 16.0 [Online], Available for download from: https://www.lazard.com/research-insights/levelized-cost-of-energyplus/, Zurich, Switzerland, 2023.
Musial, W., Heimiller, D., Beiter, P., Scott, G., and Draxl, C.: 2016 Offshore Wind Energy Resource Assessment for the United States. Technical Report NREL/TP-5000-66599. Available from: https://www.nrel.gov/docs/fy16osti/66599.pdf p 88 accessed 16 July 2020, 2016.
Optis, M., Bodini, N., Debnath, M., and Doubrawa, P.: New methods to improve the vertical extrapolation of near-surface offshore wind speeds, Wind Energy Science, 6, 935-948, 2021.
Pichault, M., Vincent, C., Skidmore, G., and Monty, J.: Characterisation of intra-hourly wind power ramps at the wind farm scale and associated processes, Wind Energy Science, 6, 131-147, 2021.
Pinson, P., Chevallier, C., and Kariniotakis, G. N.: Trading wind generation from short-term probabilistic forecasts of wind power, IEEE transactions on Power Systems, 22, 1148-1156, 2007.
Potisomporn, P., and Vogel, C. R.: Spatial and temporal variability characteristics of offshore wind energy in the United Kingdom, Wind Energy, 25, 537-552, 2022.
Pryor, S., Barthelmie, R. J., Bukovsky, M. S., Leung, L. R., and Sakaguchi, K.: Climate change impacts on wind power generation, Nature Reviews Earth & Environment, 1, 627-643, 2020a.
Pryor, S. C., and Barthelmie, R. J.: Comparison of potential power production at on- and off- shore sites, Wind Energy, 2001:4, 173-181, 2002.
Pryor, S. C., Nielsen, M., Barthelmie, R. J., and Mann, J.: Can satellite sampling of offshore wind speeds realistically represent wind speed distributions? Part II: Quantifying uncertainties associated with sampling strategy and distribution fitting methods, Journal of Applied Meteorology, 43, 739-750, 10.1175/2096.1, 2004.
Pryor, S. C., Conrick, R., Miller, C., Tytell, J., and Barthelmie, R. J.: Intense and extreme wind speeds observed by anemometer and seismic networks: An Eastern US case study, Journal of Applied Meteorology and Climatology, 53, 2417-2429, 10.1175/jamc-d-14-0091.1, 2014.
Pryor, S. C., Letson, F. W., and Barthelmie, R. J.: Variability in wind energy generation across the contiguous USA, Journal of Applied Meteorology and Climatology 59, 2021-2039, 10.1175/JAMC-D-20-0162.1, 2020b.
Pryor, S. C., Barthelmie, R. J., and Shepherd, T. J.: Wind power production from very large offshore wind farms, Joule, 5, 2663-2686, 10.1016/j.joule.2021.09.002, 2021.
Pryor, S. C., Coburn, J. J., Barthelmie, R. J., and Shepherd, T. J.: Projecting Future Energy Production from Operating Wind Farms in North America: Part 1: Dynamical Downscaling, Journal of Applied Meteorology and Climatology, 62, 63-80, 10.1175/jamc-d-22-0044.1, 2023.
Sharmar, V., and Markina, M.: Validation of global wind wave hindcasts using ERA5, MERRA2, ERA-Interim and CFSRv2 reanalyzes, IOP Conference Series: Earth and Environmental Science, 606, 012056, 2020.
Shrestha, B., Brotzge, J. A., and Wang, J.: Evaluation of the New York State Mesonet profiler network data, Atmospheric Measurement Techniques, 15, 6011-6033, 2022.
Simão, H., Powell, W., Archer, C., and Kempton, W.: The challenge of integrating offshore wind power in the US electric grid. Part II: Simulation of electricity market operations, Renewable Energy, 103, 418-431, 2017.
Smith, D. A., Harris, M., Coffey, A. S., Mikkelsen, T., Jørgensen, H. E., Mann, J., and Danielian, R.: Wind lidar evaluation at the Danish wind test site in Høvsøre, Wind Energy, 9, 87-93, 2006.
Solbrekke, I. M., Kvamstø, N. G., and Sorteberg, A.: Mitigation of offshore wind power intermittency by interconnection of production sites, Wind Energy Science, 5, 1663-1678, 2020.
St. Martin, C. M., Lundquist, J. K., and Handschy, M. A.: Variability of interconnected wind plants: correlation length and its dependence on variability time scale, Environmental Research Letters, 10, 044004, 2015.
Staffell, I., and Pfenninger, S.: The increasing impact of weather on electricity supply and demand, Energy, 145, 65-78, 2018.
Stehly, T., and Duffy, P.: 2020 Cost of Wind Energy Review, Golden, CO: National Renewable Energy Laboratory. NREL/TP-5000-81209. https://www.nrel.gov/docs/fy22osti/81209.pdf, 77, 2022.
Stensrud, D. J.: Importance of low-level jets to climate: A review, Journal of Climate, 9, 1698-1711, 1996.
Stull, R. B.: Practical Meteorology: An Algebra-based Survey of Atmospheric Science, Univ. of British Columbia, ISBN: 978-0-88865-283-6, 940 pp., 2017.
Troen, I., and Lundtang Petersen, E.: European Wind Atlas, Roskilde: Risø National Laboratory, 656 pp., 1989.
U.S. Department of the Interior: Clean Energy Future, https://www.doi.gov/priorities/clean-energy-future, 2021.
U.S. White House: FACT SHEET: President Biden to Catalyze Global Climate Action through the Major Economies Forum on Energy and Climate, https://www.whitehouse.gov/briefing-room/statements-releases/2023/04/20/fact-sheet-president-biden-to-catalyze-global-climate-action-through-the-major-economies-forum-on-energy-and-climate/, 2023.
Wilks, D. S.: Statistical methods in the atmospheric sciences, International geophysics series, Academic Press. ISBN: 9780123850225, Oxford, UK, 2011.
Wiser, R. H., Bolinger, M., Hoen, B., Millstein, D., Rand, J., Barbose, G. L., Darghouth, N. R., Gorman, W., Jeong, S., and Mills, A. D.: Land-Based Wind Market Report: 2021 Edition, Lawrence Berkeley National Lab.(LBNL), Berkeley, CA (United States). Available from: https://www.osti.gov/biblio/1818277, 88, 2021.
Zeng, J., and Qiao, W.: Support vector machine-based short-term wind power forecasting, 2011 IEEE/PES power systems conference and exposition, Phoenix, AZ, USA, 2011, 8, doi: 10.1109/PSCE.2011.5772573,

Supplemental Materials for

Quantitative Comparison of Power Production and Power Quality Onshore and Offshore: A Case Study from the Eastern U.S.

~~Onshore and Offshore Wind Resources and Operating Conditions in the Eastern U.S.~~

Rebecca Foody[1], Jacob Coburn[1], Jeanie A. Aird[2], Rebecca J. Barthelmie[2] and Sara C. Pryor[1]

[1]Department of Earth and Atmospheric Science, Cornell University, Ithaca, 14850, United States
[2]Sibley School of Mechanical and Aerospace Engineering, Cornell University, Ithaca, 14850, United States

Correspondence to: Sara C. Pryor (sp2279@cornell.edu)

The following page contains the Spearman correlation coefficients computed from 10-minute power production estimates for the IEA 15 MW reference wind ~~s~~turbine derived using LiDAR wind speeds collected at 17 NYSM stations onshore in the state of New York and on two buoys in New York Bight (offshore). The location abbreviations are as defined in Table 2 and shown in Figure 1 of the main text.

Supplemental materials. Table 1. Spearman spatial correlation coefficients of the wind power production between the 2 NYSERDA buoys and the 17 NYSM stations. Cells are color coded to aid legibility using the following classes: white [0.8, 1], yellow [0.6, 0.8), orange [0.4, 0.6], red [0.2, 0.4], and purple [0, 0.2].

	AL.	BE.	BR.	BU.	CH.	CL.	EH.	JO.	OW.	QU.	RE.	STA.	STO,	SU.	TU.	WA.	WE.	H. N.	H. S.
ALBA	1	0.541	0.349	0.368	0.510	0.416	0.371	0.509	0.576	0.420	0.570	0.412	0.405	0.404	0.488	0.373	0.402	0.283	0.275
BELL	0.541	1	0.297	0.590	0.601	0.497	0.338	0.644	0.574	0.366	0.434	0.409	0.333	0.435	0.506	0.349	0.616	0.160	0.219
BRON	0.349	0.297	1	0.259	0.334	0.310	0.621	0.344	0.366	0.783	0.359	0.750	0.696	0.713	0.431	0.714	0.343	0.523	0.463
BUFF	0.368	0.590	0.259	1	0.372	0.635	0.281	0.584	0.487	0.310	0.335	0.329	0.318	0.297	0.492	0.286	0.600	0.271	0.302
CHAZ	0.510	0.601	0.334	0.372	1	0.404	0.341	0.514	0.489	0.341	0.328	0.335	0.360	0.313	0.556	0.308	0.445	0.282	0.294
CLYM	0.416	0.497	0.310	0.635	0.404	1	0.308	0.584	0.591	0.332	0.286	0.357	0.340	0.322	0.476	0.312	0.577	0.266	0.288
EHAM	0.371	0.338	0.621	0.281	0.341	0.308	1	0.349	0.378	0.657	0.386	0.621	0.764	0.618	0.418	0.719	0.342	0.657	0.579
JORD	0.509	0.644	0.344	0.584	0.514	0.584	0.349	1	0.654	0.378	0.379	0.386	0.393	0.389	0.558	0.345	0.681	0.288	0.307
OWEG	0.576	0.574	0.366	0.487	0.489	0.591	0.378	0.654	1	0.407	0.466	0.430	0.428	0.412	0.520	0.389	0.563	0.342	0.340
QUEE	0.420	0.366	0.783	0.310	0.341	0.332	0.657	0.378	0.407	1	0.444	0.807	0.765	0.707	0.429	0.786	0.359	0.561	0.532
REDH	0.570	0.434	0.359	0.335	0.328	0.286	0.386	0.379	0.466	0.444	1	0.414	0.436	0.457	0.364	0.376	0.322	0.287	0.281
STAT	0.412	0.409	0.750	0.329	0.335	0.357	0.621	0.386	0.430	0.807	0.414	1	0.704	0.703	0.417	0.735	0.378	0.520	0.501
STON	0.405	0.333	0.696	0.318	0.360	0.340	0.764	0.393	0.428	0.765	0.436	0.704	1	0.680	0.429	0.771	0.402	0.609	0.556
SUFF	0.404	0.435	0.713	0.298	0.313	0.322	0.618	0.389	0.412	0.707	0.457	0.703	0.680	1	0.422	0.655	0.348	0.455	0.418
TUPP	0.488	0.506	0.431	0.492	0.556	0.476	0.418	0.558	0.520	0.429	0.364	0.417	0.429	0.422	1	0.398	0.508	0.364	0.329
WANT	0.373	0.349	0.714	0.286	0.308	0.312	0.719	0.345	0.389	0.786	0.376	0.735	0.771	0.655	0.398	1	0.349	0.630	0.574
WEBS	0.402	0.616	0.343	0.600	0.445	0.577	0.342	0.691	0.563	0.359	0.322	0.378	0.402	0.348	0.508	0.349	1	0.292	0.302
H. Nor.	0.283	0.160	0.523	0.271	0.282	0.266	0.657	0.288	0.342	0.561	0.287	0.520	0.609	0.455	0.364	0.630	0.292	1	0.834
H. Sou.	0.275	0.219	0.463	0.302	0.294	0.288	0.579	0.307	0.340	0.532	0.281	0.556	0.556	0.418	0.329	0.574	0.302	0.834	1